# Bolomètres : résultats et espoirs

N. CORON

# *BOLOMETRES REFROIDIS A T < 100 m K : DETECTEUR DE PARTICULES ET DE RADIATIONS IONISANTES*

extraits d'articles résumant et /ou accompagnant l'exposé de N.CORON du 6 décembre 1991 à l'Ecole d'automne d'Aussois.

1 Introduction
2 Bolometre composite et détection de la matiere noire
3 Principe d'opération et thermodynamique
Ultimes performances
4 Senseur thermistor Ge dopé :optimisation,effet du champ magnétique,puissance de charge
5 Description d'un instrument complet
6 Résultats récents :alphas,e-,X,gammas....

(extraits d'articles à créditer à leurs auteurs)

## 1. Introduction

The measurement of radioactivity by the direct conversion of nuclear radiation into the temperature rise of a calorimeter is an idea as old as nuclear physics itself [1]. However, at room temperature the sensitivity of calorimetric measurements limits these to relatively intense radiation fields, in the 1 mW range [2].

Simon [3] was the first to anticipate the enormous gain in sensitivity possible at low temperatures where heat capacities vary as $T^3$. As early as 1935 he tested a calorimeter cooled to 50 mK for radiation dosimetry measurements. In 1977, Dalmazzone [4] investigated a calorimeter at about 2.2 K and reached a sensitivity of $10^{-9}$ W. But it is only recently that the possibility of measuring with bolometers the transient temperature rise due to the detection of a single event has been analyzed [5,6] and demonstrated [7–9].

In the last few years bolometer performance in terms of mass and resolution has progressed by orders of magnitude [10–18]. Bolometers have several intrinsic advantages:

(a) the energy deposited by the radiation in an absorber is converted into heat with greater than 95% efficiency in about 1 μs;

(b) the quanta of thermal energy (or phonons) are in the $10^{-4}$–$10^{-5}$ eV range, allowing far better statistically-limited resolution than standard detectors [2,19];

(c) they have no window or dead layer;

(d) extremely good resolution can be foreseen by reducing the temperature.

Composite bolometers can now compete with standard detectors in several fields of radiation metrology: for example, a resolution of 12 eV (FWHM) for $^{55}$Fe 6 keV X-rays has been obtained with a mosaic array by the Goddard group [11] while large mass bolometers (24 g) with a resolution better than 1 keV on the base line are being developed (fig. 5 and ref. [17,18]).

Comparison of the analysis of theoretical and practical limits with recent results provides hope for an improvement of at least one order of magnitude in mass, speed and resolution in the near future. Also, new bolometers with both thermal and quantum sensors are under development (cf. fig. 8 and refs. [20,21]). These will make it possible to determine the nature of the event and, by amplification in the target, to reach lower thresholds.

Thus, two major limitations encountered in the field of ionizing radiation metrology, i.e., energy resolution and energy detection thresholds, may be improved by one or two orders of magnitude by using composite bolometers cooled to very low temperatures and operating in the pulse mode (single event mode). The

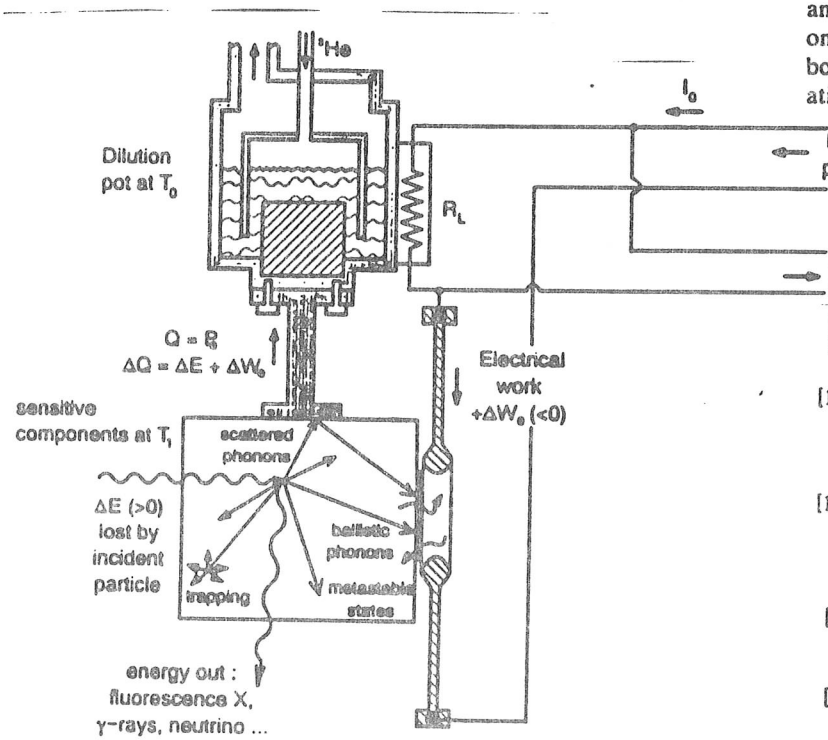


Figure 1 - Schematic diagram of a composite bolometer and of energy balance when an incident particle looses ΔE by collision on the target.


[1] P Curie and A.C. Laborde, Cr. Hebd. Séanc. Acad. Sci. Paris 136 (1903) 673.

[2] G.F. Knoll, in: Radiation Detection and Measurement (Wiley, 2nd ed., 1989) p. 688.

[3] F. Simon, Nature 135 (1935) 763.

[4] J. Dalmazzone, Rapport CEA-R-4858 (1977).

[5] E. Fiorini and T.O. Niinikoski, Nucl. Instr. and Meth. 224 (1984) 83.

[6] S.H. Moseley, J.C. Mather and D. McCammon, J. Appl. Phys. 56 (1984) 1257.

[7] D. McCammon, J.C. Mather and R.F. Mushotzky, J. Appl. Phys. 56 (1984) 1263.

[8] N. Coron, G. Dambier et al. Nature 314 (1985) 75.

[9] H. Stroke, G. Artzner, et al. IEEE Trans. Nucl. Sci. NS-33 (1986) 759.

[10] N. Coron, P. de Marcillac et al. in: The Quest for the Fundamental Constants in Cosmology, eds. J. Andouze and J. Tran Thanh Van (Editions Frontières, 1990) p. 275.

[11] D. McCammon, B. Edwards et al. in: Low Temperature Detectors for Neutrinos and Dark Matter III, eds. L. Brogiato, D.V. Camin and E. Fiorini (Editions Frontières, 1990) p. 213.

[12] S.H. Moseley, R.L. Kelley, R.J. Scholkopf, A.E. Szymkowiak, D. McCammon and J. Zhang, IEEE Trans. Nucl. Sci. NS-35 (1988) 59.

[13] D. McCammon, W. Cui et al. to be published (1991); and Paper XVII-1, Massachusetts at Int. Conf. on Particles and Nuclei, June 25–29 (1990). ●● please update●●

[14] A. Alessandrello, C. Brofferio, D.V. Camin, O. Cremonesi, E. Fiorini, A. Giuliani, G. Pessina and E. Prentali, Nucl. Instr. and Meth. A289 (1990) 504.

[15] P.F. Smith, G.J. Homer, S.P.J. Read, D.J. White, J.D. Levin and N.J.C. Spooner, Phys. Letters B245 (1990) 265.

[16] J.W. Zhou, O. Redi et al. communication to the Am. Phys. Soc. 22 April 1991; and Bull. Amer. Phys. Soc. 36 (4) (1991) 1301.

[17] P. de Marcillac, N. Coron et al. Proc. 2nd DAEC Meeting, 5–8 March, 1991.

[18] P. de Marcillac, N. Coron et al., submitted to Physics Letters (1991).

[19] H.H. Andersen, Nucl. Instr. and Meth. B15 (1986) 722.

[20] A. Cummings, N. Wang et al. IEEE Trans. Nucl. Sci. NS-38 (1991) 226.

[21] P.N. Luke, J. Appl. Phys. 64 (1988) 6858; and P.N. Luke, J. Beeman, F.S. Goulding, S.E. Labov and E.M. Silver, Nucl. Instr. and Meth. A289 (1990) 406.

## 2 COMPOSITE BOLOMETERS AND DARK MATTER DETECTION

A large proportion of the mass in the universe may be under the form of non baryonic particles weakly interacting with matter (W.I.M.P.)[17-21]. Present detection of these particles can be attempted only with germanium[22] or silicon detectors[24] in which only about 25 % of the recoil energy can be transformed into an electrical current.Observing recoil energies smaller than 5 KeV is nearly hopeless. Moreover these detectors have few non-zero spin nuclei, so that the interaction rate is expected to be very low for certain particle candidates such as the photino (see 17, 18, 19). Massive composite bolometers have potentially several advantages :

- the material of the target can be chosen among several possibilities, as LiF, $TiO_2$, $Cr_2O_3$ ...A set of composite bolometers with different targets can help to determine the nature of the interacting particles ;
- the ultimate resolution depends essentially on temperature and can be in the 10 eV range for a 1 kg low heat capacity single crystal cooled below 10 m°K ;
- the quanta of thermal energy modes (phonons) are in the $10^{-3}$-$10^{-4}$ eV range,so that intrinsic statistical noise is very low (≈ 0.3 eV on a 100 eV recoil energy !).

The collision between a dark matter particle (with mass $m_X$) and a nucleus (with mass $m_N$) of the target deposits in the bolometer a recoil energy E, the average value of which is [21] :

$$< E > \approx 2\ \text{KeV}\ \frac{m_N}{1\text{GeV}}\left[\frac{m_X}{m_N + m_X}\right]^2 \qquad (1)$$

For $m_X$ = 5 GeV and for $^{27}Al$ with $m_N$ = 25 GeV we get < E > = 1.4 KeV.

Because of the three times better recoil energy detection efficiency and of the better matching of masses, a 1 KeV (nominal threshold) LiF bolometer will detect cosmions of 2.6 GeV while a 1 KeV (nominal threshold) classical Ge detector[22] will detect only cosmions with mass above 12 GeV. Bolometers with diamond, germanium, silicon or sapphire targets are now classical ones.All hard single crystals will work as well. For an absorber with bad thermal properties a composite-sandwiched target can be a solution as we proposed earlier[10].

Interaction rates will depend strongly on the nature of the particle and of the spin of the target[17-21] .The calibration of such detectors will be possible on recoils from neutrino scattering[23] or on collimated neutrons[24]. Several groups in the world are now developing low temperature cryogenic thermal detectors for dark matter[5,20,22]. In France extensive collaborations are developing on this subject and the "Institut des Sciences de l'Univers" supports this program[25] helped also by international collaborations (N.Y. University, Göteborg University, CERN-ISOLDE). We present below our most recent theoretical and experimental results.

## 3 OPERATION AND THERMODYNAMICS OF THE COMPOSITE BOLOMETER

Present bolometer theories implicitly suppose that the whole energy is finally confined in the sensor.We think that this is not exact for the composite bolometer (except perhaps in an hypothetic ballistic phonon detector mode). The composite bolometer consists mainly of an absorber or target with heat capacity $C_a$, very well thermally connected to a sensor or thermistor with heat capacity $C_{th}$. By construction these two elements are always at nearly the same temperature $T_1$ (in the frequency bandpass of the whole bolometer). They are connected to the refrigerator by a thermal link of thermal conductance G optimised so that the thermal time constant $\tau_{th} = (C_a + C_{th})/G$ has the wanted value.

When a particle strikes the target with an absorbed energy ΔE the sensor receives a fraction of it as heat, ΔQ, with :

$$\Delta Q = \left(\frac{C_{th}}{C_a + C_{th}}\right)\Delta E \qquad (2)$$

Up to now, small bolometers had $C_{th} >> C_a$ and normal theory with ΔQ = ΔE was appropriate. But for massive bolometers a new question arises : what is the optimal $C_{th}/C_a$ ratio ? We attempt an answer : we suggest to consider the composite bolometer system as a

thermodynamic engine in which the heat reservoir is the composite sensitive part at $T_1$ and the cold reservoir is the cryostat at $T_0$. The second principle of thermodynamics states that only a fraction $\eta_t$ of heat $\Delta Q$ extracted from the heat reservoir at $T_1$ can be transformed into (electrical) work, with $\eta_t = 1 - T_0/T_1$.

The maximum useful signal that can be transferred to a measurement is thus:

$$\Delta We = \eta_t \frac{C_{th}}{C_a + C_{th}} \Delta E \qquad (3)$$

We must now reestimate the two fundamental noise sources existing in a bolometer : the thermodynamic noise and the "polarising" noise. The first noise is due to statistical fluctuations of the thermal energy in the sensor[26,28] which will be converted into noise signal with maximal efficiency $\eta_t$ ; this noise after conversion in work is $\Delta N1_{rms}$ :

$$\Delta N1_{rms} = \eta_t \sqrt{kT_1^2 C_{th}} \qquad (4)$$

where k is the Boltzmann constant.

The second noise is due to the statistical fluctuations (= $\Delta Pe_{rms}$) of the polarising power Pe which maintains the bolometer at the optimal temperature $T_1$. This noise is called either the "Johnson noise" if the sensor is electrically polarised, or the "photon noise" if the sensor is optically polarised. As long as Pe is transmitted by quanta of energy $\delta E << kT_1$ we get (demonstrated in ref.29 for photons) :

$$\Delta Pe_{rms} = \sqrt{Pe}\sqrt{kT_1}\sqrt{B} \qquad (5)$$

where B is the bandpass.

But the fraction of Pe available to change energy in the sensor is only $Pe_{th}$ with :

$$Pe_{th} = Pe \times \frac{Cth}{Ca + Cth} \text{ and } \Delta Pe_{th} = \sqrt{Pe_{th}}\sqrt{kT_1}\sqrt{B} \qquad (6)$$

We'll suppose here that power fluctuations $\Delta Pe_{th}$ are converted into signal noise $\Delta N2_{rms}$ with an efficiency equal to one (voltage fluctuations not converted into heat),while measuring energy $\Delta E$. We introduce $\tau_e$, the electrical time constant of the pulse connected to the true time constant $\tau_{th}$, by $\tau_e = \phi\tau_{th} = \phi\frac{C_a + C_{th}}{G}$ where $\varphi$ is a coefficient depending slightly on the thermistor sensitivity.Then, with optimal filtering of the signal pulse, it is demonstrated[28] that $\Delta E_{rms} = \sqrt{\tau_e}\,\Delta Pe_{rms}/\sqrt{B}$ . As applied here:

$$\Delta N2_{rms} = \sqrt{\tau_e}\,\Delta Pe_{th}/\sqrt{B} = \sqrt{Pe\frac{C_{th}}{C_a + C_{th}}} \times \sqrt{kT_1} \times \sqrt{\tau_e} \qquad (7)$$

Using $P_e = G(T_1 - T_0)$ and $\varphi = 0.5$ (typical value of good thermistors) we can simplify (7) to :

$$\Delta N2_{rms} = \sqrt{C_{th}\, kT_1 (T_1 - T_0)/2} \qquad (8)$$

Then the ultimate resolution for a composite bolometer becomes :

$$\Delta E_{rms} = \frac{C_a + C_{th}}{C_{th}} \times \frac{1}{\eta_t}\sqrt{\Delta N1_{rms}^2 + \Delta N2_{rms}^2} = \frac{C_a + C_{th}}{\sqrt{C_{th}}} \times f(T_1, T_0) \qquad (9)$$

If $C_a$ and $C_{th}$ vary as $T_1^3$ this expression goes through a minimum when

$$T_1/T_0 = \theta_m = 1.2 \qquad (10)$$

and

$$C_{th}/C_a = \psi_m = 1 \qquad (11)$$

It can be shown that this minimum is always obtained for values of $\theta_m$ around 1.2 and of $\psi_m$ around 1 independent of the rates of variation of $C_{th}$ and $C_a$ with $T_1$, or of the electrical characteristics of the sensor.

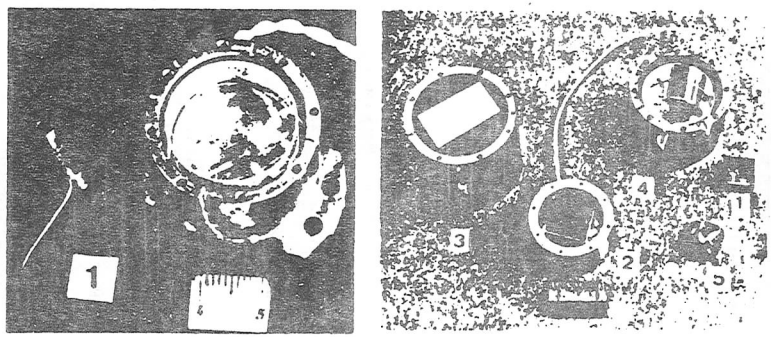


a b

Figure 2

a- A classical infrared bolometer with collecting optics compared to the 25 g bolometer for dark matter

b- Massive bolometers under construction with different materials :
Ge (1, 2, 3);Sapphire(4);Diamond(5)

So from thermodynamic considerations only, we have established that for all composite bolometers the best resolution is obtained when the thermal capacity of the sensor equals the thermal capacity of the target. This general new theorem was first demonstrated by Buhler and Umlauf in the particular case of the magnetic bolometer[11] and was generalised by us[5].

Our analysis is for the pessimistic case where no amplification exists through the sensor. If some amplification exists we obtain the same conclusions after replacing $\eta_t$ by $\eta_e = (1 - \tau_e/\tau_{th})$, but the ultimate calculated resolution would be better. This amplification mecanism may also introduce supplementary noise proportional to $\eta_t/\eta_e$. So for the dark matter detector we'll use the thermodynamic limit independent of the sensor.

Finally, the possible resolution of a composite massive bolometer optimized with $C_a = C_{th} = \frac{C_b}{2}$ at a working temperature $T_1$ and maintained by the polarising power at $T_1 = 1.2\ T_0$ is (with $\Delta E_{FWHM} = \sqrt{8 \ln 2}\ \Delta E_{rms} = 2{,}35\ \Delta E_{rms}$) :

$$\Delta E_{FWHM} = 5.7 \sqrt{k C_b(T_0) \times T_0^2} \qquad (10)$$

So, for dark matter detection,the ultimate possible resolution of a composite bolometer with a 1 kg single crystal target is :

$$\Delta E_{FWHM} = 4.2 \times 10^{-8}\ T_0^{5/2}\ \theta_D^{-3/2}\ M_A^{-1/2} \quad \text{in Joule}/\sqrt{\text{kg}} \qquad (11)$$

where $\theta_D$ is the Debye temperature and $M_A$ the atomic mass (in grams) of target material.

These ultimate performances will only be obtained if :

a the thermal gradients are minimised between sensitive parts at T1 ;

b the conversion of recoil energy into heat is complete and stable : no energy stocked in defaults, or trapped charges ;

c the current noise in the sensor is negligeable ;

d non interesting sources of energy are filtered : windows must stop infrared photons ; filters must stop electrical interferences ;vibrations must be stopped in the bandpass of the bolometer (= 10 Hz to 10 KHz) ;

e the cooling system is stable ($\frac{\Delta T}{T} < 1$ %) and with no microphonics ;

f the noise temperature of the preamplifier is less than 2 To.

Massive bolometers in the 1- kg range will necessitate a substantial volume of material for the sensor which must also be perfectly homogeneous in response. At the present time, we think that only the germanium thermistor, heavily doped by normal techniques, available in large volume, will be useful for massive bolometers with electrical polarisation.

This expression for the ultimate resolution, established for a perfectly isothermal bolometer and a perfect sensor, is approached experimentally only with the best bolometers and then by a factor varying between 4 and 60 (see table 1). From eq. (1) it can be seen that for a given mass of monocrystalline target which has a heat capacity varying as the product of mass and $T^3$ (Debye's law) the ultimate resolution varies as $m^{1/2}T^{5/2}$. Thus, in theory, extremely good resolution is possible by reducing the temperature sufficiently. As shown in fig. 2a, it is hoped to have a noise level of 1 eV (FWHM) and comparable energy resolution in a 25 g massive sapphire bolometer at 10 mK, while X-ray mosaics of mg bolometers may reach a resolution of $10^{-2}$ eV at the same temperature. The best experimental results are plotted for comparison in fig. 2a.

In practice, the bolometer is connected to the cryostat by a thermal link of conductivity $G$ (consisting of a thin strip of material) so that it is reset after each event with a time constant $\tau_e$, which in turn determines the maximum possible event rate. This electrical time constant of the bolometer at the biasing operating point is given by $\tau_e = 0.5\ C/G$, (see refs. [10,25]).

Bolometers have two major limitations:

(a) they have a very low energy threshold so that they are very sensitive to microphonics and electromagnetic pickup. This can be solved by careful design of the cryogenic system [10] and with cooled preamplifier stages [11,26].

(b) they are slow: their time constant $\tau_e$ is limited by the presently available homogeneity of sensors and increases on reducing the temperature (fig. 2b).

One possible explanation [10] for these long time constants could be the fact that the sensor must be polarized with a power $P_e$ so that $T_1 = 1.2\ T_0$; as at equilibrium $P_e = G(T_1 - T_0)$, and with $C = (C_s + C_a) \approx 2C_s$ and $\tau_e \approx 0.5\ C/G$, we see then

$$P_e = (0.2 T_0 C_s)/\tau_e \qquad (2)$$

or $P_e/C_s \approx 1/\tau_e$.

This means that to have a fast bolometer we must choose a sensor which combines high sensitivity with a high polarizing power per unit heat capacity. This explains why the trend in the development of bolometers will now be in this field [11].

The shortest time constants obtained with the presently available sensors are plotted in fig. 2b. The points indicate the best experimental results for composite bolometers. Our measurement of $P_e/C_s$ in a normally doped Ge sensor is consistent with ref. [11] where the results for an implanted silicon sensor provide hope for a factor of 17 improvement at 100 mK, and, perhaps, better than this at 10 mK, but experimental proof has yet to be obtained. In any case, a time constant in the 1 ms range is presently obtained with small and large mass bolometers that compete

Table 1
Reported energy resolutions of massive bolometers ( > 1 g). According to the author $\Delta E_{FWHM}^{meas}$ is relative either to the base line or to a spectral line $\Delta E_{FWHM}^{crystal}$ is the ultimate energy resolution of a perfect composite bolometer as given by eq. (1)

| Crystal | Mass [g] | $T_{bath}$ [mK] | Sensor | $\Delta E_{FWHM}^{meas}$ [keV] | $\Delta E_{FWHM}^{meas} / \Delta E_{FWHM}^{crystal}$ | Ref. |
|---|---|---|---|---|---|---|
| $Al_2O$ | 24 | 50 | Ge-NTD | 0.6 baseline | 4 | 17 |
| | | | | 3.7 spectral line (59.6 keV, $^{241}$Am) | 24 | |
| | 280 | 135 | Ir supra | 66 | 10 | 30 |
| | 2 | 60 | $RuO_2$ film | 38 | 540 | 31 |
| LiF | 8 | 15 | Ge | 9.4 | 1050 | 15 |
| | 32 | | | 28.2 | 1550 | 15 |
| Si | 1 | 15 | Ge | 3.5 | 1350 | 15 |
| | 4 | | | 5.9 | 1100 | 15 |
| Ge | 11 | 28 | Ge | 13 | 230 | 32 |
| | 60 | 30 | Ge-NTD | 9.4 | 60 | 20 |

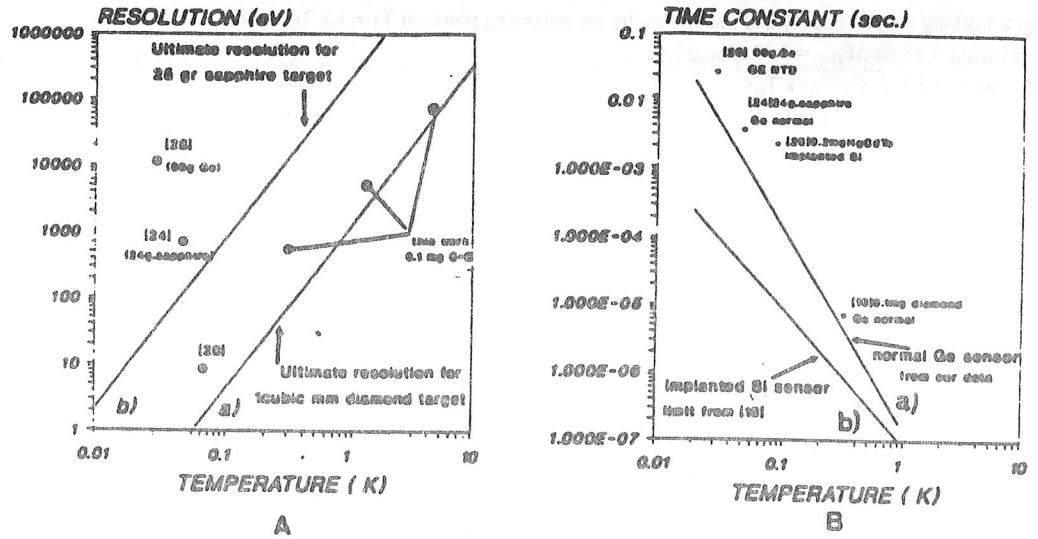


Fig. 2. (Left) Resolution of composite bolometers as a function of temperature: line a) is the ultimate resolution for small composite bolometers with a typical 1 $mm^3$ diamond target (3 mg) as a function of temperature – this is the target in the development of x-ray mosaics; line b) is the ultimate resolution possible for large-mass bolometers with a typical 6 $cm^3$ target (25 g). The points indicate resolution values obtained to date. (Right) Time constants for bolometers as a function of temperature: line a) is our estimated limited for presently available Ge sensors (normal and NTD). line b) is estimated from [11] for the implanted silicon sensor and is a goal for future development. The points indicate time constants actually obtained so far for the fastest high resolution bolometers.

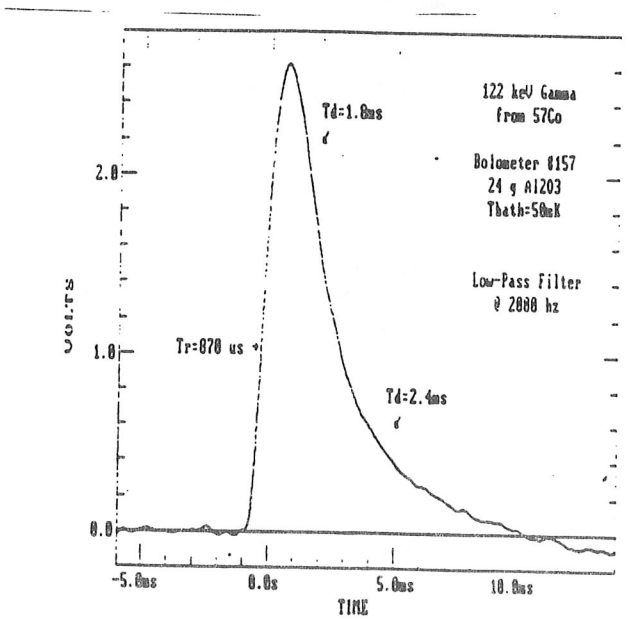


Fig. 3. Pulse shape of a 122 keV gamma-ray event in our 24 g sapphire bolometer cooled to 50 mK. The resolution on the base line is 600 eV and the time constant varies from 3 to 5 ms. The values of these parameters are the best obtained to date with large-mass bolometers by about an order of magnitude.

with standard detectors in resolution. Typical pulse shapes are presented in fig. 3 for a large bolometer and in fig. 7a for a small one. A compromise between resolution, temperature and speed should be carefully studied in terms of the applications and the sensor availability.

## 4 THE HEAVILY DOPED GERMANIUM THERMISTOR

Up to now the best results have been obtained with heavily doped semiconductor (Ge or Si) for the thermistor[5,9]. Then, at low temperature, electrical conduction comes from the "hopping" mechanism where electrical carriers jump from an occupied site to an unoccupied one with a probability increasing steeply with temperature[31,32]. The resistance varies exponentially with temperature and the difficulty is to obtain a sensor with an impedance matched to electronic and time constant constraints, typically in the 10 KΩ-100 MΩ range, at a working temperature $T_o$. For example, the resistivity at 0.1°K varies as the 140-th power of the doping concentration or of room temperature resistivity (see Figure 3).

To solve this difficulty, and make bolometers of reasonable impedance, we monitor with very high precision the resistivity of germanium wafers at 300°K with the four-probe method. We use a specially designed, low pressure, 400 μm spacing, four-point probe. At 300°K we have to measure values around 0.06 ohm.cm resistivity with a few per thousand precision. The typical map of a 15 x 15 $mm^2$ region is shown in Figure 4 for a wafer doped for 0.1°K temperatures with $\langle\rho\rangle \approx 0.052$ ohm.cm.

Resistivities of several tested thermistors (made of Ga doped Germanium) are plotted as a function of temperature in Figure 5. Curve labelled "Bol 143" is for the 25 g bolometer thermistor : there is a very sharp transition from conduction to non-conduction at 80 ± 20 m°K, typical of good doping homogeneity and of a measurement without parasitic background in the sensor.

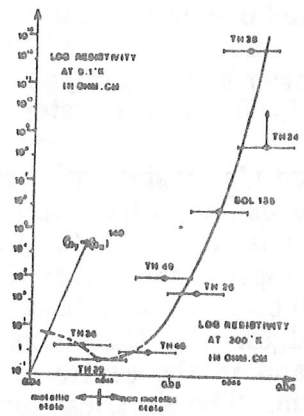


Figure 3
Resistivity of heavily doped germanium thermistors measured at 0.1°K as a function of room temperature resistivity (T = 298°C). Large error bars are due to errors on size measurements.

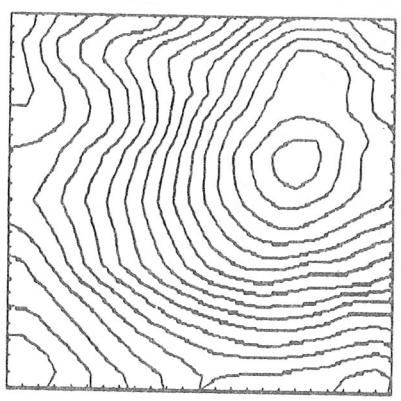


Figure 4 - Resistivity maps of a 15 x 15 $mm^2$ slice of heavily doped Ge ; resistivity varies 5 per cent around 0.05 ohm cm between top and bottom ,corresponding to three orders of magnitude at 0.1° K. This map needed 100 hours of robotic measurement

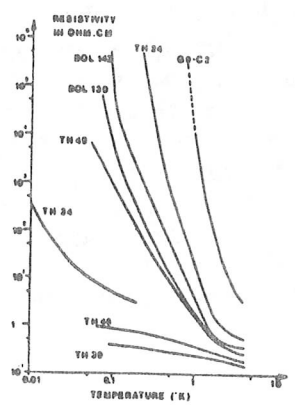


Figure 5 - Resistivity of typical doped Ge sensors as a function of temperature below 4°K

# Puissance de charge acceptable par unité de volume et Adaptation d'impédance par le champ magnétique (*) !

Sous champ magnétique $\vec{B}$ les orbites des électrons se déforment et deviennent elliptiques toutes dans la même direction : la probabilité de leur interaction diminue et le matériau devient isolant. D'où les premières mesures de senseurs de bolomètres sous champ magnétique font pour demontrer la possibilité d'adapter l'impédance d'un même bolomètre à différentes températures :

---

In a first experiment towards a bolometric system for high resolution particle detection a Ga doped Ge thermistor was tested. We measured the resistance as a function of temperature in externally applied magnetic fields up to 8 Tesla. Our main interest was whether the thermistor resistance could be tuned using the magnetoresistance effect. Secondly, the power handling capability with respect to the nonlinear I–V characteristics is important for future bolometer use in magnetic fields.

---

The thermistor TH–43 is a heavily Ga doped Ge crystal with very low compensation ($K < 3$ %), especially Czochralsky pulled for us [5]. It has approximate dimensions of 5 x 1.5 x 1.5 mm$^3$ and a room temperature resistivity of 0.0512 Ωcm, which is close to the metal–semiconductor transition at an approximate resistivity of 0.045 Ωcm [6]. The crystal has four electrical contacts : two current contacts at both outer edges, and two voltage contacts at 0.5 mm from the edges. The thermistor was attached to the cold finger of the $^3$He–$^4$He dilution unit and in the centre of the superconducting magnet with a homogeneity of $10^{-4}$ over 1 cm. The electrical connections are made by

---

a four–wire strip thermally anchored at several temperatures. Outside the cryostat a connection is made through a well shielded cable to a home made constant current source with a range of 2 nA to 40 μA and an analog Keithley 155 Volt meter with a sensitivity of 0.1 μV. Both are operated on batteries and enclosed in a small faraday cage to reduce noise pickup in the system which might cause some heat–up of the thermistor. For the same reason, we put capacitors where the leads enter the cryostat and also at the Volt meter and current source input. In this way, we obtain a low pass filter and suppress high frequency noise in the system. Temperatures below 100 mK are measured using a $^{60}$Co(Co) nuclear thermometer. A calibrated $RuO_2$ thermometer, with a field independent resistance even at high fields, is used for higher temperatures.

## I–V characteristics

At several points between 550 mK and 5 mK and for different fields ranging from 0 to 8 Tesla we bias the sample with different currents I and measure the voltage V over it. Typical I–V curves are shown in fig. 1 . At low currents we observe a linear ohmic behavior where V = I.R ( with R the resistance ), while at higher currents we obtain a saturation of the output voltage. It seems that all thermistors show the same behavior, i.e. they become non–linear above a certain electrical power input V.I at low temperatures. Possible physical origins for this phenomenon are : 1) an electric field dependence of the conductivity due to a non–uniform distribution of impurities [7] and 2) the hot electron or electron–phonon decoupling effect. In the second model, it is argued that the electrons and the lattice of the sample at low temperatures are only weakly thermally coupled [8].

* From P de Moor et al Oxford 1991 to be published

We would like to propose another non-linear effect. At low temperatures the heat conduction in heavily doped Ge itself is very bad [9] such that temperature gradients might occur over the crystal. The resistance is lower at the warmest part of the crystal so the current will mainly flow through there and, dissipating its electrical power, will locally warm it even more. So one measures the resistance of the warmest path through the thermistor. At high power there can be a substantial difference between the temperature of that region and the temperature of the cold finger ! Moreover, bad heat transport at very low temperatures through the glue or epoxy, which are used for electrical isolation, might create even larger temperature gradients between current path and cold finger.

A preliminary interpretation of our data indicates that the observed non-linearity is caused by a combination of effects : a rather large electric field effect but also a thermal effect. As a quasi non-dissipative thermometry technique, nuclear orientation offers the possibility to check the lattice temperature at several places in the thermistor using different nuclear sources. In this way one can learn whether electron-phonon decoupling or temperature gradients are responsible for the thermal part of the non-linear behavior.

The problem of using thermistors in a bolometer is that the thermometer sensitivity $A = d\log R/d\log T$ decreases considerably in the non-linear region. To obtain an optimal signal to noise ratio, a bolometer must be sufficiently polarised to have a temperature rise of 12 % [2]. It has been indicated that only very slow bolometers are possible if the handling power is too low [1]. To optimize thermistors, one is interested in the power handling capability per volume $P_c/V$, which is defined as the power injection per volume unit which causes a resistance drop of 30 %. In our sample at 80 mK the critical power $P_c$ is approximately 9 $\mu$Watt. Saturation of the I-V curve above this limit can be seen in fig. 1. The higher $P_c$, the higher bias current one can use for read-out without loosing sensitivity. In fig. 2 $P_c/V$ is plotted for different fields and temperatures. At $T \geq 100$ mK, $P_c$ is almost field independent whereas at lower temperatures $P_c$ decreases with increasing field B. However $P_c$ might depend on the absolute resistivity or on the temperature sensitivity, which are both much higher for example at 6 Tesla. For a thermometer, $P_c.A$ should then be maximized. For a bolometer – absorber plus thermistor – a maximum value for

$P_c.A/C$ (with C the heat capacity of the whole system) should give the best results. Anyway, the presently measured $P_c$ are equal or higher than previous zero field measurements on NTD or chemically doped Ge with equivalent A value [2][8].

## 2.3 Resistance versus temperature

The sample resistance $R = V/I$ taken at low current (i.e. well below the critical power) versus the cold finger temperature is plotted in fig. 3 for different magnetic field values. For temperatures above 20 mK the resistance seems to follow qualitatively a

$$R \sim T^{-A}$$

law which does not correspond with the variable range hopping law

$$R = R_0.e^{(T_0/T)^{\frac{1}{4}}}$$

However, at larger fields ($\geq 4$ T) and $T \geq 20$ mK a steeper increase from the resistivity versus temperature is suggested from the data, which can be described with this formula. A possible physical explanation may be the fact that the sample is not far from the metallic state. At low fields and at low temperatures a partially metal and semiconductor current path is followed. This would cause the resistance to be lower than expected. At higher fields, the effective distance for the conduction electrons between one dopant and another is larger. Then the sample will be more semiconductor-like than metal-like. In a way one is able to change the sample from a rather metallic state to a more semiconductor state by adjusting the magnetic field. From the point of view of a "detectorologist", we are mostly interested in the thermometer sensitivity A which varies from $A = 1/3$ at zero field to $A = 4$ at 8 Tesla. Thus the detector sensitivity increases a factor 12 with the field !

The R(T) dependence at $T \leq 20$ mK shows a saturation of R. This might indicate that the sample remains at a temperature of 20 mK even when the cold finger is at a lower temperature. The reason for this might be RF-heating or another parasitic power coming in, a non-ideal thermal contact to the sample holder at these temperatures, or temperature gradients in the crystal itself (due to parasitic power or radiation heating), as suggested above in section 2.1 .

## Resistance versus field

We find a drastic increase of resistance by changing the external field. At e.g. 20 mK the zero field resistance is 55 Ω where at 6 T it is 1.4 MΩ, which is almost 5 orders of magnitude difference ! Taking into account the extrapolated 1 GΩ at 20 mK and 8 T, we have 7 orders of magnitude difference between 0 and 8 Tesla at 20 mK, and 2 orders of magnitude at 550 mK. In fig. 4 the resistance is plotted against $B^2$. For fields above 2 T

$$R \sim e^{\beta B^2}$$

gives a good description while for lower fields the resistance R seems to increase even faster with increasing field B.
This shows that an external magnetic field is a powerful and flexible method to change the resistance of thermistors. If one wants to operate at a certain temperature (at a suitable time constant of the bolometer for example) R can be changed with B to reach an optimal impedance for the read–out electronics.

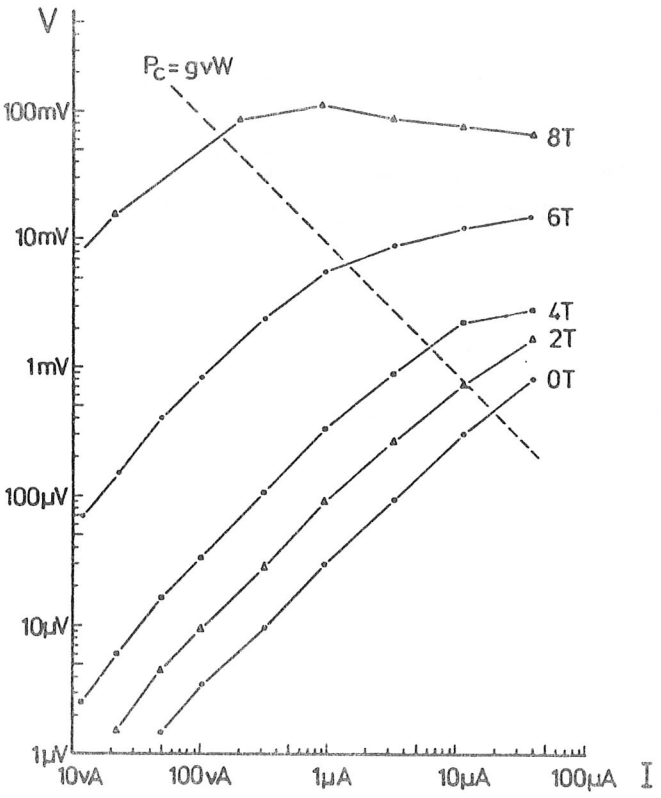


Fig. 1 : Typical I–V curves for different field values taken at 80 mK. Above the critical power $P_c$ of 9 aW saturation of the voltage is visible.

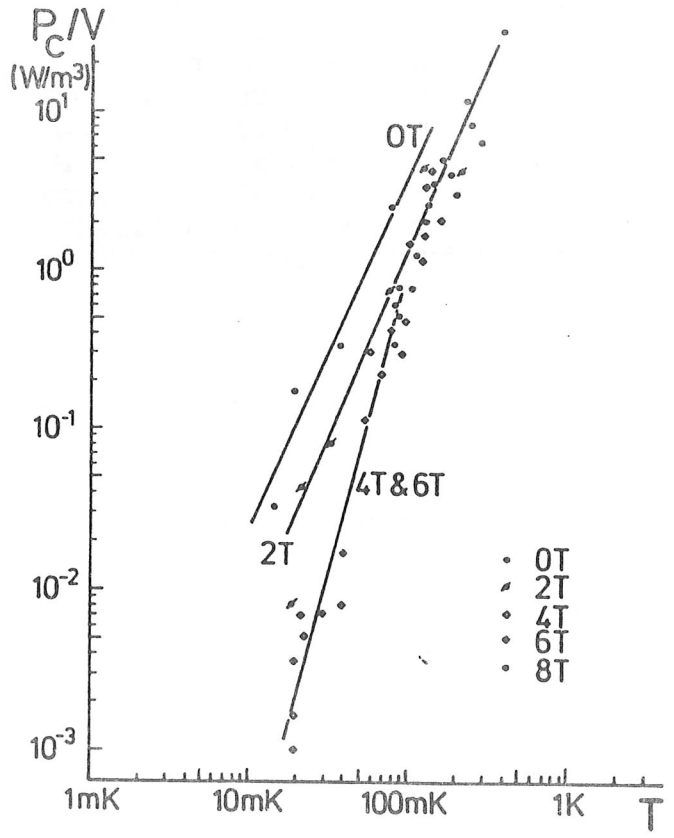


Fig. 2 : Power density $P_c/V$ required to reduce the resistance by 30 %, as a function of temperature and magnetic field.

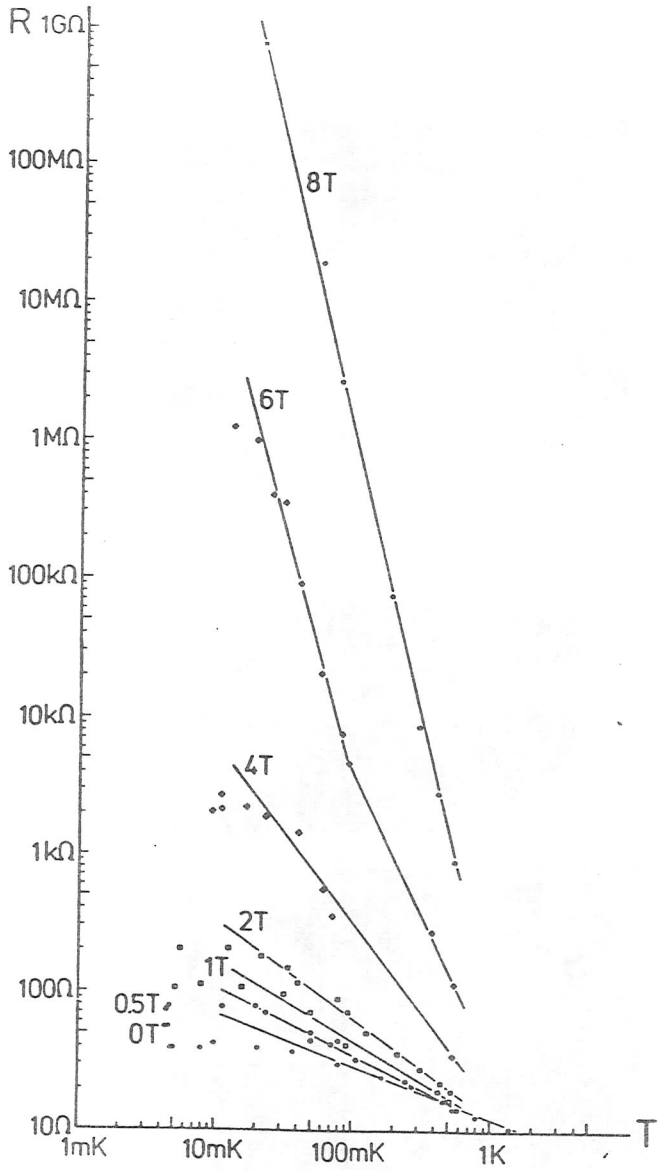


Fig. 3 : The resistance R as a function of temperature and magnetic field. The 8 Tesla 1 GΩ point (x) is an extrapolated value at 20 mK.

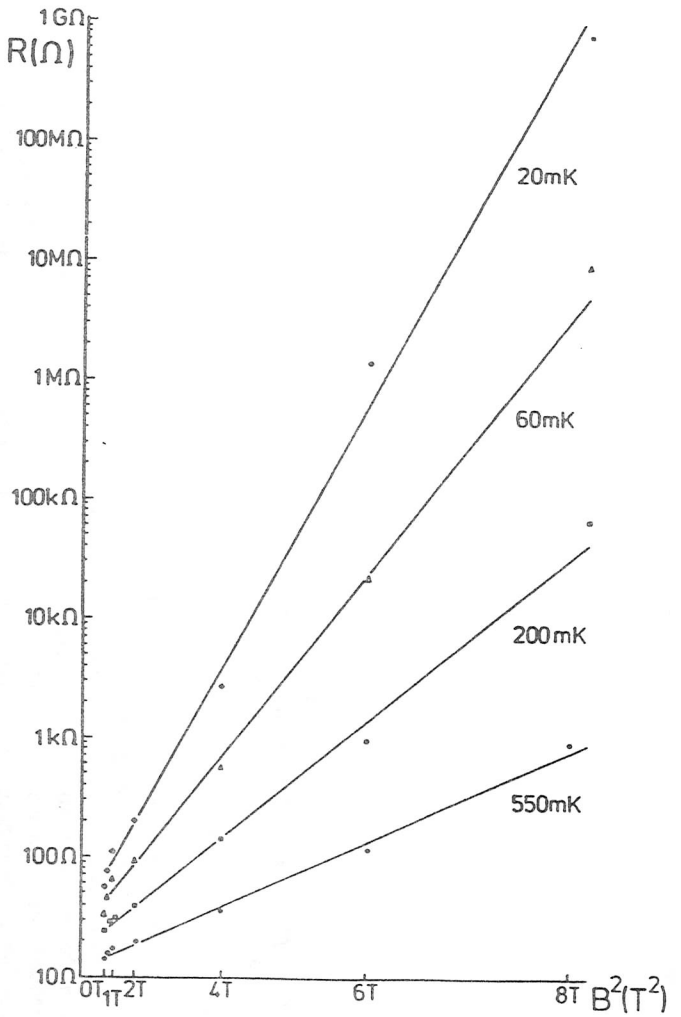


Fig. 4 : The resistance R as a function of $B^2$ for different temperatures.

V

## Description of the complete instrument for thermal spectrometry

To operate, bolometers must be cooled to a temperature low enough to reach the required resolution. With a standard portable $^4$He cryostat and a compact adsorption $^3$He refrigerator [27], it is possible to work for up to 48 hours at 0.3 K with small bolometers ($\approx$ a few mm$^3$) and to obtain resolutions in the 500 eV range with X rays and electrons or a few keV with ions [26]. The spectrum in fig. 7 was obtained with such an instrument. But it is at temperatures equal to or below 100 mK that bolometers can truly compete with more standard techniques. Thus, several groups are now working on the development of complete instruments for space or terrestrial applications below 100 mK. For large-mass bolometer measurements we use an inexpensive commercial dilution system (from TBT-Airliquide France) operating at an ultimate temperature at 50 mK: it has an outside diameter of 45 mm so that it can be used in a standard $^4$He container (see fig. 4).

Microphonic problems become crucial for resolutions below 200 eV with small bolometers and below 10 keV with those of large mass. All our results (figs. 5, 6 and 7) have been obtained with rather old refrigerators not at all intended for bolometry. Our group and others are preparing a new generation of dilution refrigerators with two order of magnitude less microphonic noise power.

Bolometers are also sensitive to the continuous background and this may change their response with time. Thus the design of the instrument must ensure excellent stability of the vacuum around the bolometer since the latter may act also as a manometer, being sensitive to the thermal energy of impinging molecules. Shields will protect the bolometer from background and random infrared radiation. The connections between the bolometer and the preamplifier must be carefully protected from all electromagnetic pickup and vibration. The temperature noise of the electronics at the bolometer impedance must be lower than the temperature noise of the bolometer itself (which is very close to twice the bath temperature [25]).

Commercial preamplifiers have an equivalent temperature noise $T_n$ of around 300 mK at 200 Hz and a special input stage with a cooled junction field-effect transistor (JFET) must be used to go below this. We obtain a $T_n$ of around 50 mK at 40 MΩ impedance in our laboratory with a J230 transistor. The Goddard group claims 5 mK temperature noise at 20 MΩ [11] with "an inexpensive JFET cooled at 130 K".

To eliminate electromagnetic pickup problems we use batteries for the preamplifier supply and optical-fiber connections to the data acquisition system (a 1 MHz, 12 bits ADC and a 32 bits microcomputer).

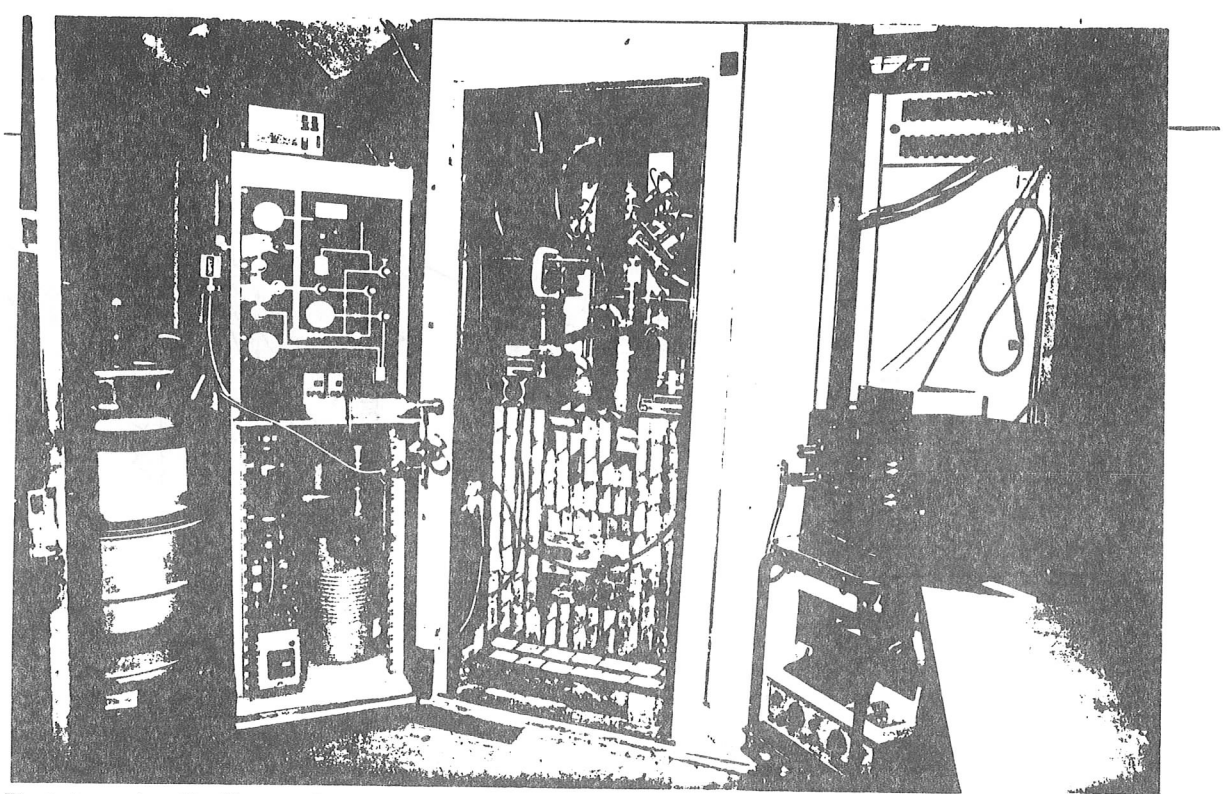

Fig. 4. A complete 50 mK system for tests with internal X-ray sources or external gamma-ray sources; performances reached on the base line are: 40 eV resolution with small bolometers and 600 eV with large bolometers. In this case the system is arranged for low-level radioactivity measurements, with a 20 cm lead shield to reduce the background (the Faraday cage cover and the microphonics shield have been removed for the photograph).

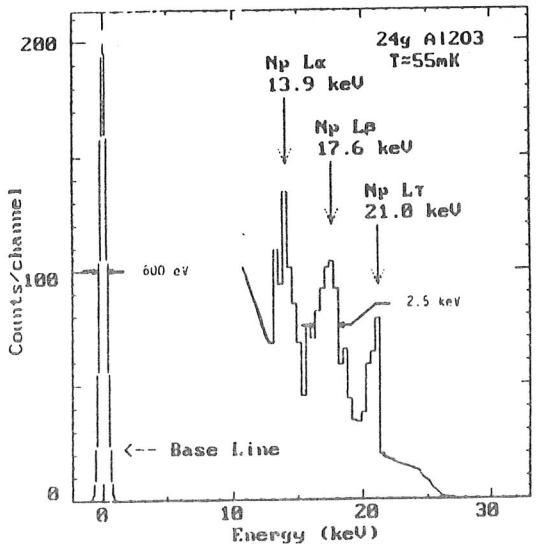


Fig. 5. Photon spectrum from a $^{241}$Am source obtained with a 24 g sapphire bolometer (area 310 mm$^2$) cooled to 55 mK and positioned in the refrigerator shown in fig. 4.

## Experimental results

We have recently obtained the best resolution to data measured in the large-mass bolometer detection of gamma-rays and high-energy alpha particles, i.e., 2.5 keV for the 18 keV L X rays of $^{241}$Am (fig. 5 and [17,18]) and 10.5 keV for 6 MeV alpha particles (fig. 6). The Goddard–Wisconsin group has published, for a single, selected detector, a resolution of 7.5 eV for the $^{55}$Fe 6 keV X rays [13]. The best results that we and other groups have obtained for the bolometric detection of different ionizing radiations are summarized in tables 1 and 2.

Generally, measured resolutions depend, as in standard detectors, on the energy $E$ and on the nature of the radiation: (a) For low energies (where $(E/\Delta E) < 50$) the situation is simple: the resolution $\Delta E$ (FWHM) is found to be independent of $E$ in most cases. (b) But for high energy for $E/\Delta E > 50$ we may have variations of the response of the bolometer with impact point or time that degrade the resolution: heat propagation

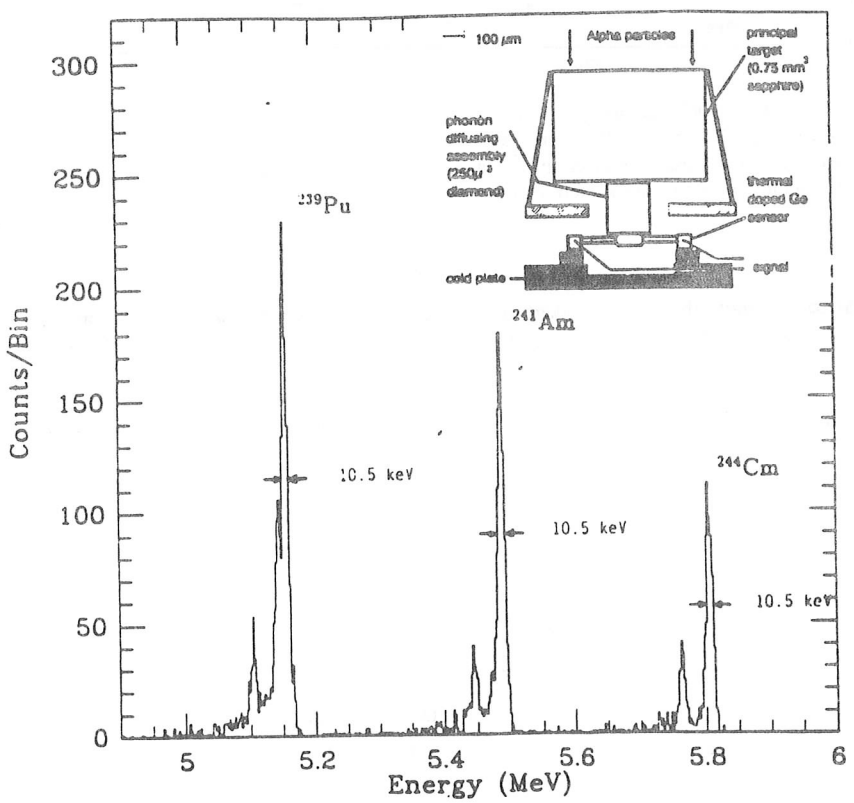


Fig. 6. Spectrum of a commercial mixed alpha source ($^{239}$Pu, $^{241}$Am, $^{244}$Cm) obtained with a composite-composite bolometer (see inset) of our design. The New York University refrigerator, modified to reduce microphonics, was operated at 60 mK but the bolometer was set by polarization at 380 mK to obtain the best response stability. The resolution is better than 11 keV.

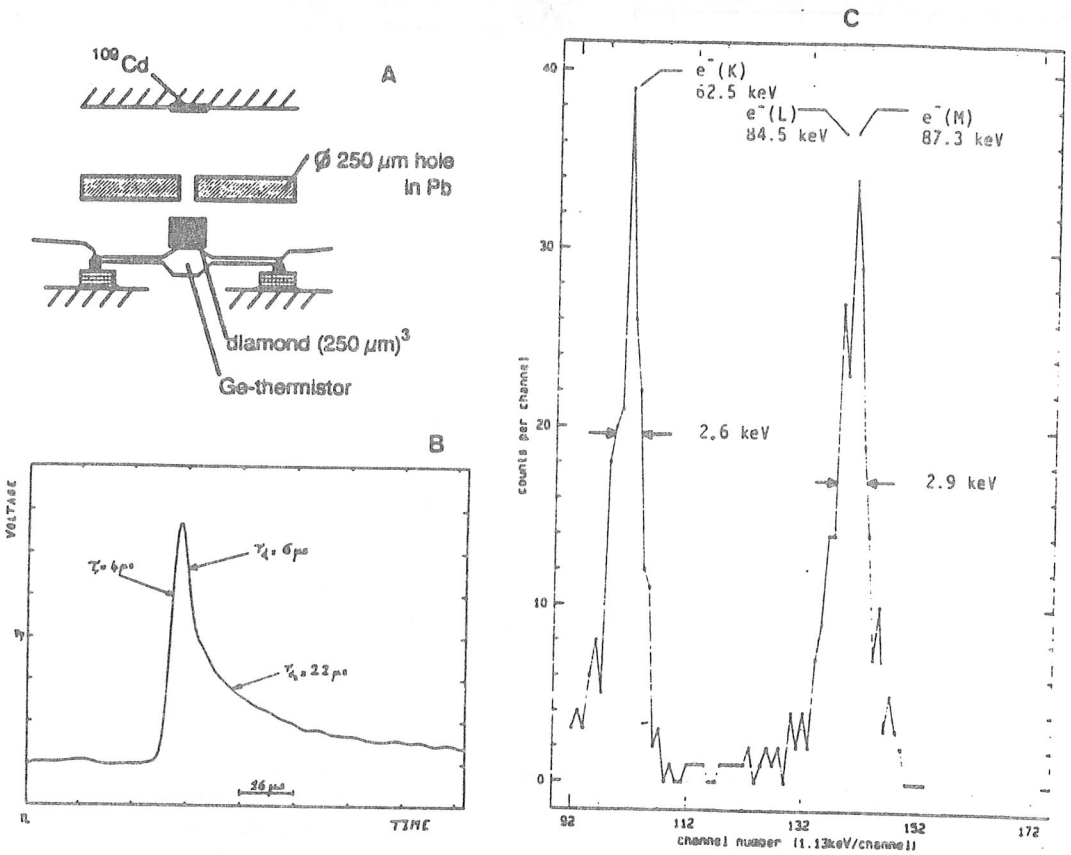


Fig. 7. Test of a small bolometer at 300 mK using electrons: (a) the composite diamond bolometer and the $^{109}$Cd conversion electron sources. (b) a typical pulse for an 84 keV electron showing the short time constant (6 μs) and a tail due to the heat link capacity effect or an internal sensor diffusivity effects. (c) $^{109}$Cd conversion electron spectrum. In this test the resolution is limited to 3 keV by the microphonics associated with the nitrogen shield and poor $^3$He temperature stability.

depends on the distance between the impact point in the target and the sensor. As the sensor is not homogeneous and as ballistic phonons (with a few percent of $E$) travel along particular directions, this yields gives a response which depends on the impact point: this appears clearly for gamma rays absorbed very close to the sensor if the target is not thick enough.

This is the reason why the composite-composite bolometer was designed [16]. In this device the heat after being diffused is transmitted more homoge-

Table 2
Resolution of composite bolometers compared with that of conventional quantum detectors

| Ionizing particle (energy) | Quantum detectors $\Delta E_{FWHM}$ | Composite bolometers | | | |
|---|---|---|---|---|---|
| | | published performances | | | Realistic goal for near future $\Delta E_{FWHM}$ |
| | | $\Delta E_{FWHM}$ | mass and target material | ref. | |
| X-ray (6 keV) | 120 eV, Si (Li) | 7.5 eV | ≈ 0.2 mg, HgCdTe | [13] | 3 eV |
| gamma-ray (≈ 20 keV) | ≈ 1 keV, Hp-Ge | < 2.5 keV | 24 g, $Al_2O_3$ | this work | |
| (1332 keV) | 1.6 keV | 13 keV | 11 g, Ge | [32] | |
| β or e⁻ (≈ 80 keV) | ≈ 2 keV, Si(Li) | 3 keV | 0.1 mg, diamond | this work | 200 eV |
| α (≈ 5 MeV) | 9 keV, IPS | 10.5 keV | 3 mg, $Al_2O_3$ | this work | 3 keV |

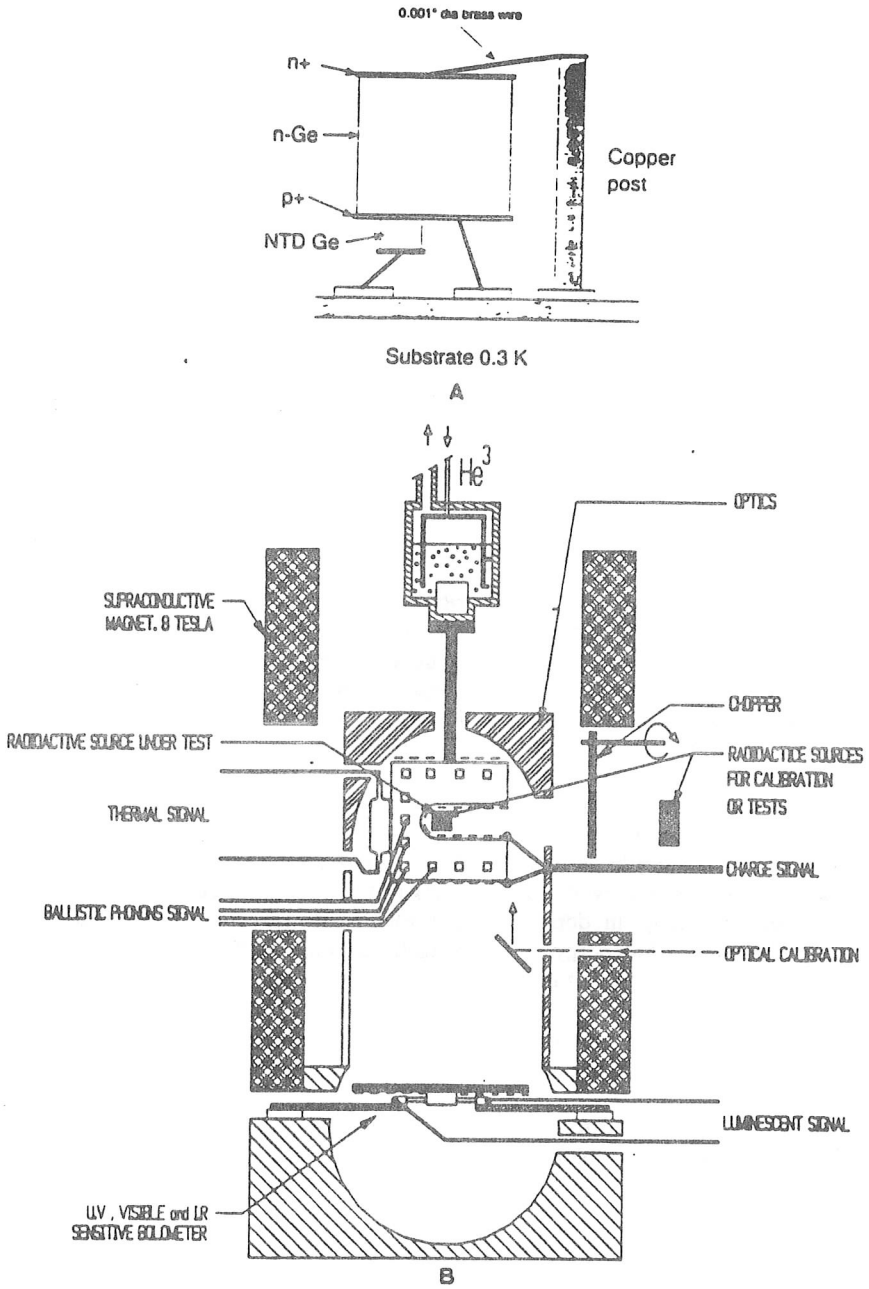


Fig. 8. Towards the "optimal" radiation detector where quantum and thermal effects are measured to yield maximum information. (Top) Design of the voltage-assisted calorimetric detector successfully tested by Luke et al. [21,22]. (Bottom) Prospective design of the future optimal bolometer where all the information related to an event is used. In this design (1) a thermal sensor measures the heat (75% of energy), (2) a charge signal measures ionization in the target, if it is made of semiconducting material ≈ 20% of energy), (3) ballistic phonon sensors measure the impact parameters (direction and position ≈ 2% of energy), (4) an optical bolometer with uniform response to UV and IR measures the fluorescence ( ≈ 3% of energY). A superconducting magnet allows crossing the metallic–nonmetallic transition in the thermal sensor so that it can be adjusted to the optimal impedance at each temperature. This design will provide: (a) a lower threshold by amplification in the target, (b) identification of the nature of the event, (c) better pileup rejection and time correlation, (d) discrimination of microphonic noise.

neously to the sensor (see fig. 6). This new design makes it possible to achieve 10.5 keV resolution with 6 MeV alpha particles. We hope in the future to approach the ultimate limits calculated by Andersen [19] for ions and alpha particles (a limit of about 2 keV for alpha particles) and due to the energy stored in defects.

The response of the bolometer may also vary with time for extraneous reasons; eg change in the refrigerator temperature, "manometer" effect, microphonics, ... . These effects are easily eliminated by the proper design of the cryogenic system. If the refrigerator has sufficient cooling capacity the best way is to reduce its temperature $T_0$ and to use a higher than theoretical polarization in the bolometer, so that it is maintained at a temperature $T_1$ with $T_1/T_0 > 4$. We are then under high-stability conditions with respect to variations in $T_0$ and out-gassing effects.

It has now been demonstrated by our group [16] and the Goddard–Wisconsin group [12] that a resolving power $E/\Delta E$ of better than 500 is possible for several hours with bolometers.

## 5. Possible improvements and applications in ionizing radiation metrology

By using a more complex bolometer design (as shown schematically in fig. 8) it will be possible to have a better energy efficiency and more information for each event. Indeed, when a particle or photon impinges on the target its energy is not completely degraded into heat immediately: from about 100 ns to 3 μs we have: ionization (25% of the energy event in silicon), fluorescence (≈ 3% of the energy in doped crystals) and ballistic phonons (≈ 3% of the energy in pure crystals). By adding new sensors on or around the target it should be possible to detect these signals and use this information for precise arrival time measurements, localization of events [28] or any discrimination [20,29].

Work on the simultaneous detection of fluorescence and heat has started in France [29]: a second bolometer, sensitive to optical radiation as shown in fig. 8b will detect the fluorescence signal with a sensitivity of $10^{-16}$ W/(Hz)$^{1/2}$, nearly as good as a photomultiplier. We hope, by measuring the fluorescence to thermal signal ratio, to be able to identify the event (recoil or ionization) and so eliminate most of the thermal noise signals in low level radioactivity measurements.

It should be noted, that achievement of the stated performance in X- and gamma-ray, beta- and alpha-particle spectrometry with composite bolometers should be very important for improving the knowledge and the accuracy of the nuclear data needed in ionizing radiation metrology.

In the same way it is also possible to amplify the thermal signal. Very promising results have been obtained with the voltage-assisted calorimetric ionization detector (fig. 8a) first developed by Luke in 1988 [21]. His idea is a new approach to detection that combines the calorimetric and ionization measurement techniques. The principle was demonstrated with a bolometer operating at 1.8 K with a HPGe (5 mm$^3$) diode as absorber, and a neutron transmuted doped (NTD) Ge thermistor as the temperature sensor. In this design the amount of ionization generated by an event on the detector is measured by the heat produced by the charged carriers as they drift across the detector under an applied bias voltage instead of by the direct measurement of the charge itself.

This result in a greatly amplified thermal signal. Luke et al. [22] claim that with this technique it may be possible to achieve electronic noise levels lower than the signal arising from a single pair of carriers and propose applications of these detectors in astrophysics research.

Although it is not yet possible with the present results from this new type of voltage-assisted calorimetric detector to reach a definitive conclusion regarding their potential it has appeared important for the LPRI to be associated with the study of these devices and to consider applications that could result in progress in ionizing radiation metrology. Even if the energy resolution of this type of detector is ultimately limited by the statistics of the ionization process (see [21]), the interest is evident in the field of integral counting for absolute activity measurements ($4\pi$ measurements, $4\pi$ beta-gamma coincidence measurements, ...). The lowering of the detectable energy threshold to a value of a few eV would make the extrapolation to zero energy (which may be one of the principal source of error in this field), negligible. Work is in progress.

These steps towards the ideal bolometer provide hope for significant applications of thermal detection to several fields of radiation metrology in the future.

# Simultaneous Measurement of Ionization + Phonons

## 60 g Berkeley

Sadoulet et al
Oxford
09/91

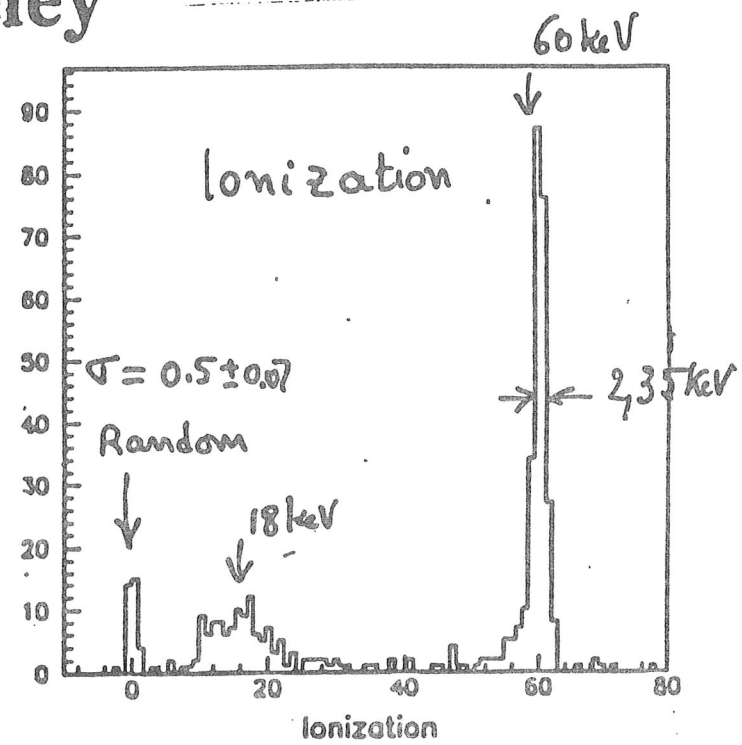


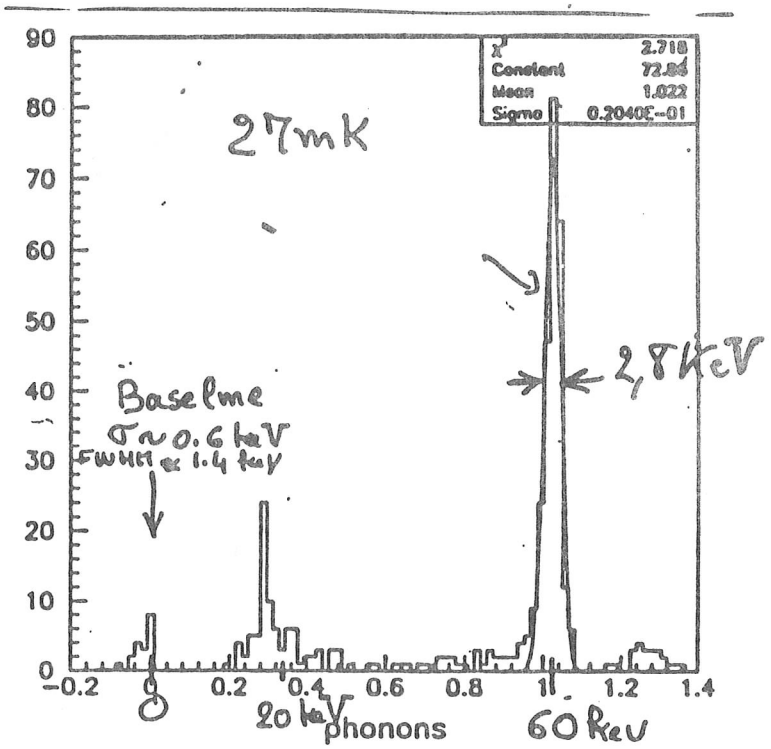


Detection simultanée des charges N de la chaleur dans 60 g de Ge refroidi à 27 m°K par Sadoulet et al. à Berkeley.

Resultats obtenus avec un bolomètre saphir de 24g : *

*A low threshold achieved with a 24 g sapphire bolometer.*
In the continuation of our previous work with massive sapphire crystals, we designed a new 24g bolometer. The dilution system was operated at its lowest reachable temperature, i.e. 50 mK. Compared to the previous 25g sapphire [4] [5], the thermal coupling between the sensor and the crystal has been modified: heat is allowed to reach both sides of the sensor, of reduced size, with lower thermal

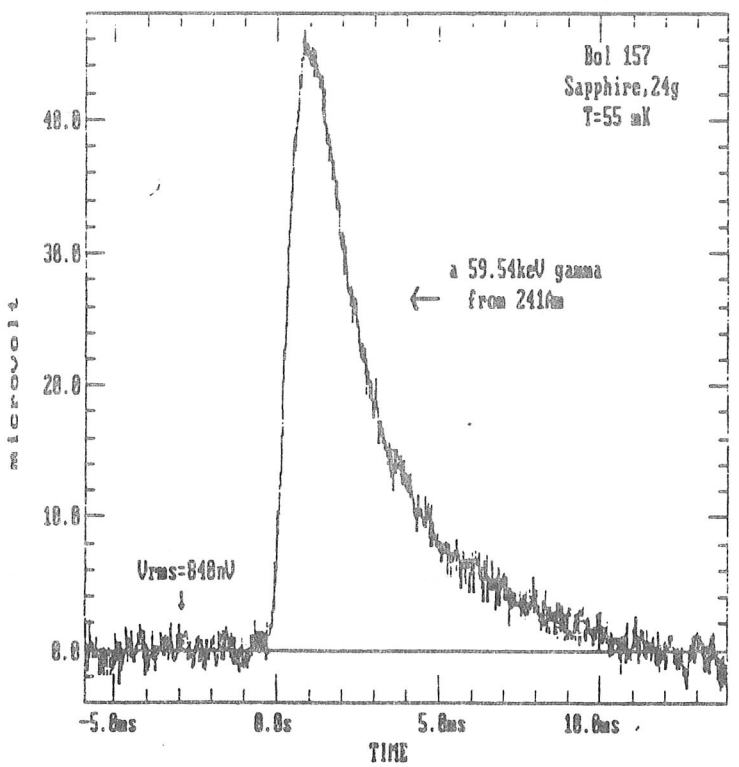


Fig. 4: A typical 59.54 keV gamma from $^{241}$Am as seen by a 24g sapphire bolometer, cooled at 55mK. Time constants are $t_{rise}$ ~ 870 $\mu$s and $t_{decay}$ ~ 5.2ms.

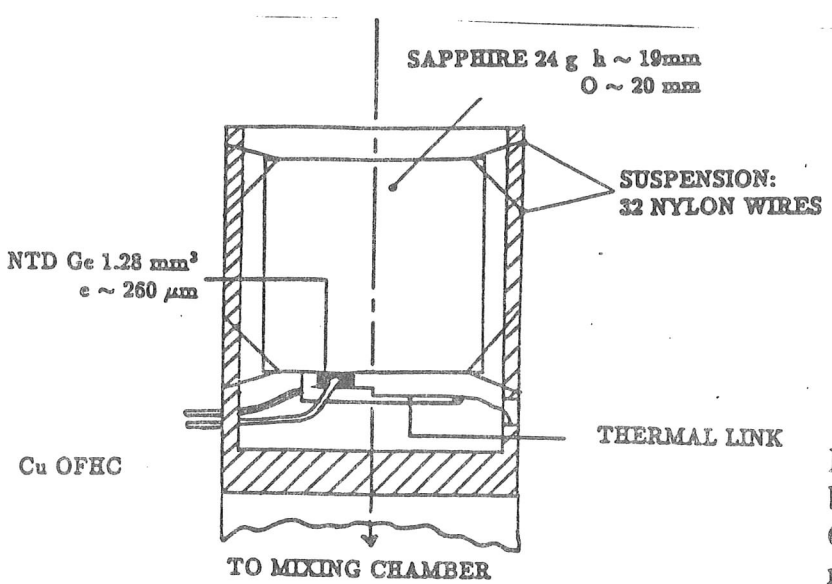


Fig. 3: Design of a 24g $Al_2O_3$ bolometer, with a 1.28 mm$^3$ NTD Ge glued on it. Heat is allowed to reach both sides of the sensor

* P de Marcillac et al Oxford 1991

gradients, and increased speed as a result. We used the same support as before with 32 nylon wires, and a thin sapphire strip as thermal leak (Fig.3).
A typical 59.6 keV gamma from an $^{241}$ Am source, as seen by this bolometer at the operating point, is shown unfiltered in Fig. 4. A 30 min long experiment was stored using a 12 bits ADC oscilloscope connected to the preamplifier via an optical fiber. Optimising the filter with respect to signal to noise ratio, this record shows a 3.7 keV FWHM resolution on the 59.6 keV line, while a 600 eV FWHM width on the base line is observed (Fig.5). Note that different approaches were tried for filtering, but none of them was able to reduce the width of the line. A simple low frequency pass filter, with a cut off at $f \sim 350$ hz, gave the best result. The width of the base line was deduced from the sampling of the pretrigger base line of each event, once filtered. This was resumed in a more than $10^6$ points histogramm.
The trigger level was set at about 12 keV during this run. We were able to record events of lower energy in a second one, with no trigger (2600 events in 1 min active

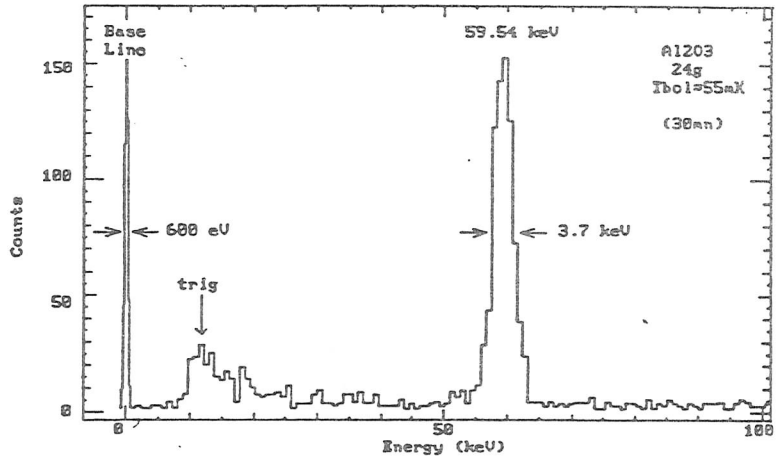


Fig. 5: Gamma spectrum of the 59.54 keV line of $^{241}$Am recorded by a 24g sapphire bolometer at $T \sim 55$mK. Band pass filtering 3hz-350hz

time). Such an event is plot in Fig. 6 using a 26 times magnification to give the same height as a 59.6 keV gamma. We can thus conclude that a 2.3 keV event is easily detected by this bolometer. This is the first evidence of a threshold around 1 keV obtained with a massive bolometer.
The temperature dependence of our NTD germanium sensor is given in Fig. 7. Compared to published data [6], these measurements indicate a doping concentration of about $8.10^{16}$ atoms Ga/cm$^3$. At the operating point $i \sim 4$ nA; $R = 3.2$ MΩ and $dR/RdT \sim 140$ K$^{-1}$. We tried to check the Debye's law for sapphire, i.e. the $T^3$ dependence of the specific heat. Assuming the validity of our previous measurements on doped Ge we deduced the (dynamic) heat capacity of sapphire at 55 mK.

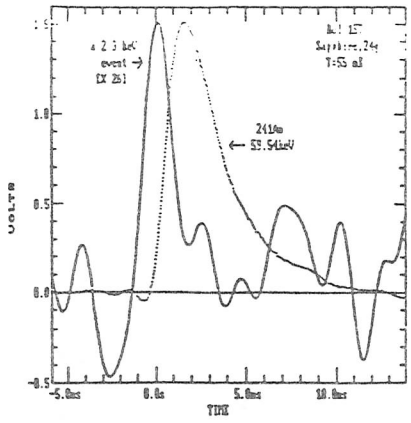


Fig. 6: A low energy event recorded by a 24g $Al_2O_3$ bolometer at $T \sim 55$mK. A typical 59.54 keV is overplot, and a 26 magnification was applied to the low energy event to determine its energy. Band pass filtering 3hz-400hz

This point is shown in Fig. 8 with previous experimental data [1, 4, 7, 8]. A relative agreement is found with Debye's law, assuming a good fit at "high" temperature. Our last point at 55 mK and 95 mK are even lower than the expected values: we may have overestimated the contribution from the Germanium, which would be a sign of a bad thermalisation. However the comparison of the same event as seen by the previous 25g bolometer and the new one is instructive (Fig.9). Gains in both

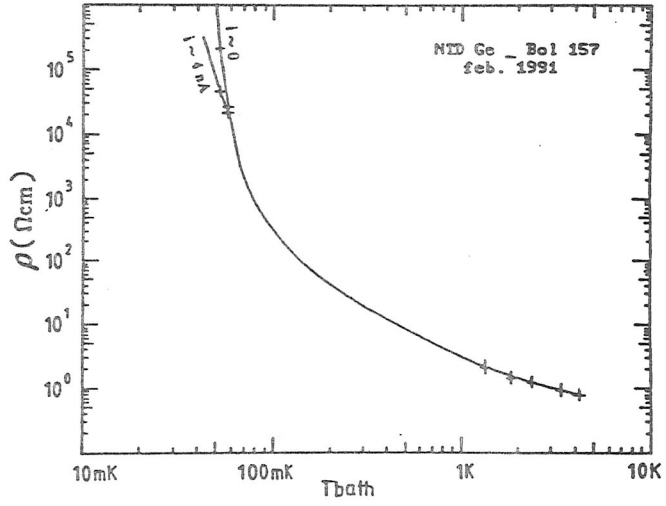


Fig. 7: Resistivity dependence with the bath temperature of the 1.28 mm$^3$ NTD Ge sensor used with the 24g sapphire bolometer

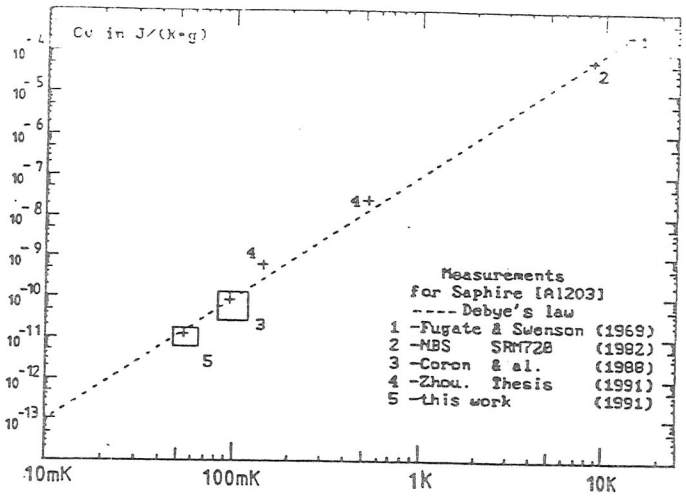


Fig. 8: Specific heat of sapphire in $JK^{-1}g^{-1}$ from our measurements. The Debye's law is extrapolated from measurements at "high" temperature

signals (x7.5), attributed to the lowest temperature, and speed (x5), which may be due to the reduced size of the sensor, are achieved. Taking $\Delta E_{FWHM\ ultimate} \sim 8\ (kT^2_{bath}\ C_{crystal})^{1/2} \sim 180$ eV as a realistic estimation of the ultimate sensitivity of our bolometers, we mesure only a four times greater level on the base line; so

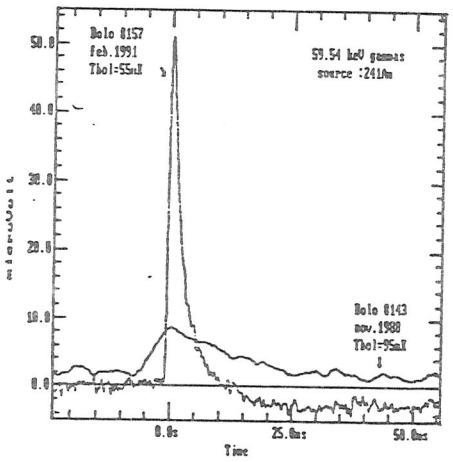


Fig. 9: Comparison of a 59.54 keV event from $^{241}$Am as seen by two massive $Al_2O_3$ bolometer. Bolo # 143 (25g) was cooled at 95mK, while bolo # 157 (24g, this work) was cooled at 55mK

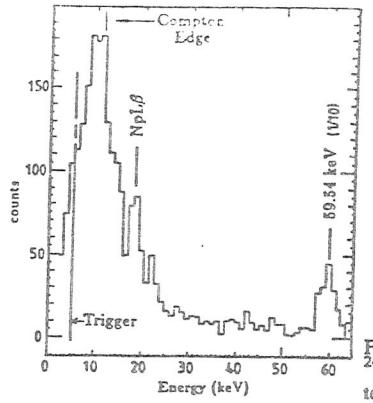


Fig. 10: Low energy part of the gamma spectrum of $^{241}$Am in a 24g sapphire bolometer. Only one over ten 59.54 keV gamma was recorded

that only small improvements are expected if we do not change the whole design of the experiment.
Contributions to the noise level were estimated to give the following classification with decreasing magnitudes: non isothermal effects in the sensor; amplifier noise; Johnson noise; thermodynamical noise. Adding these different contributions, we found a noise level close to the measured one, so that we certainly had very few

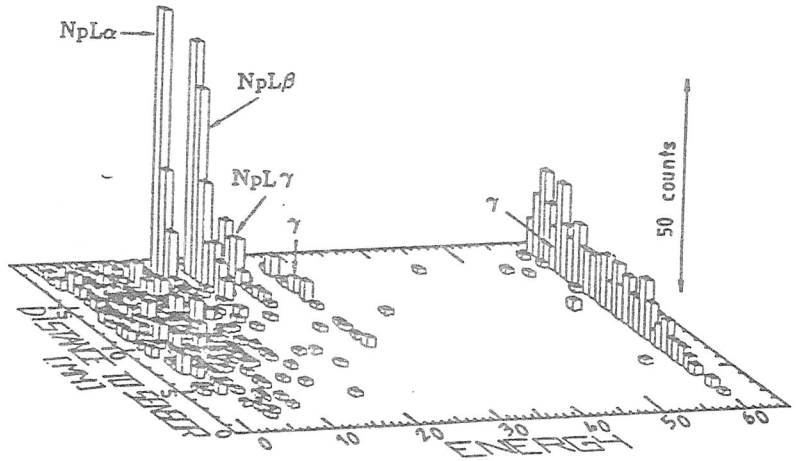


Fig. 11: Simulation of the mean location of energy deposit in a 24g $Al_2O_3$ bolometer from an $^{241}$Am source

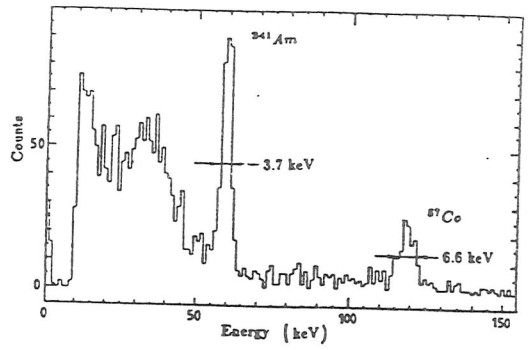


Fig. 12: Gamma spectrum of $^{57}$Co (external source) and $^{241}$Am (internal source) recorded by a 24g sapphire bolometer at 55mK

microphonics in this run. In fact this bolometer approaches theoretical limits at 100 mK, where it is nearly isothermal during a pulse event; but at 50 mK gradients appear, so that we expect better performances at this temperature by using a thinner sensor of equal volume.

Focusing on the X ray lines of $^{237}$Np and using the 59.6 keV line as calibration, a resolution better than 2.5 keV FWHM is measured on the 17.6 keV NpL$\beta$ line (Fig.10). The high event rate at low energy could be atributed to the Compton scattering events from the 59.6 keV line, as shown by a Monte-Carlo simulation of the experiment. This simulation presents a greater dispersion of the 59.6 keV

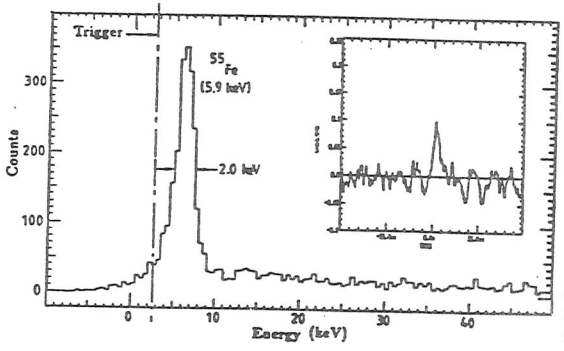


Fig. 13: X ray spectrum of $^{55}$Fe (5.89keV) as seen by a 24g sapphire at 55mK. A typical event is shown in the inset. Duration: 5 hours. The trigger is set by software to 2.55keV. Shielding:20cm Pb + 13mm Cu.

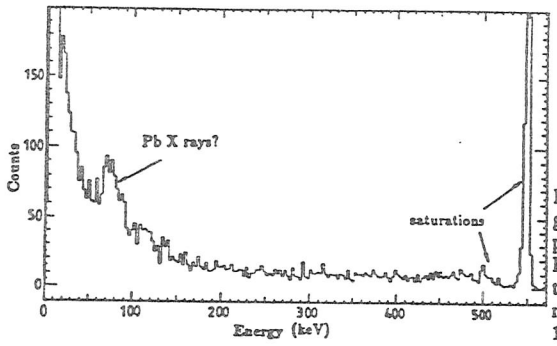


Fig. 14: Low energy background recorded by a 24g sapphire bolometer at 55mK. Duration: 2h45. The peak at the right is for amplifier's saturation. Shielding: 20 cm Pb + 13mm Cu

events within the crystal compared to the low energy lines (Fig.11). This might be responsible of the discrepancy between the base line and the full line width. We plan a further experiment to check it. A spectrum obtained with an external $^{57}$Co source shows all the expected features of 122 keV $\gamma$'s interaction with the crystal (Fig.12).

In order to make measurements of the low energy background, we decided to remove the internal $^{241}$Am source, and to replace it by a $^{55}$Fe source, which

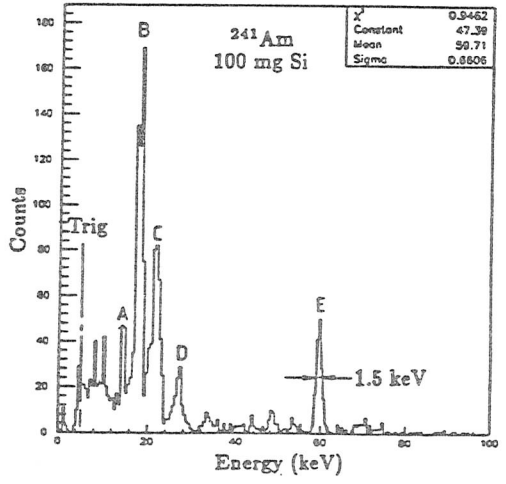


Fig. 15: Gamma spectrum of $^{241}$Am in a 100mg Si bolometer at $T$ ~ 60mK. We recognize all the features of the expected spectrum. A: NpL$\alpha$ (13.9keV), $\Delta E_{FWHM}$ ~ 800eV; B: NpL$\beta$ (17.6keV); C: NpL$\gamma$ (21.0keV); D: $\gamma$ (26keV); E: $\gamma$ (59.6keV), $\Delta E_{FWHM}$ ~ 1.5keV. An optimal filtering was applied

suppressed the Compton distribution of the previous spectrum. A crude shielding was used (20 cm Pb + 13 mm OFHC Cu) for this experiment. Unfortunately, we noticed an added specific heat, which we attributed to a thin superfluid helium film deposit on the bolometer which came from a microleak in the calorimeter vacuum. This reduced the sensitivity to about 0.2 its previous value, and the resolution on $^{57}$Co was then only 17 keV FWHM. Nevertheless, we could observe the 5.89 keV events at the expected event rate, during a 5 hours run. The FWHM resolution on the 5.89 keV line, far above the "software set" trigger at 2.55 keV, is about 2.0 keV, while we had then only 1.8 keV FWHM on the base line (Fig.13). Moreover, the background at 10 keV was estimated to about 3.5 $10^4$ evts.keV$^{-1}$.kg$^{-1}$.day$^{-1}$, at least four orders of magnitude higher than the requirements for D.M experiments(Fig.14). We note an enhancement of the background around 80 keV, which could be due to Pb X rays. The integrated event rate above 10 keV was about 40 events.s$^{-1}$.kg$^{-1}$, this is at least 10 times higher than the upper internal radioactivity level deduced from low background measurements of sapphire made with germanium detectors at both LPRI and at the Frejus tunnel. We are confident that this event rate will be reduced, using a better shielding unless there is some internal $\beta$ source in the sapphire.

Prospects.

The stimulating results obtained keep us rather confident that we have nearly a detector in hand for a pilot experiment at the Frejus laboratory. We intend to use the 24g sapphire crystal to study the radioactivity from cryostat and shielding.
A 100 mg silicon bolometer, tested at 65 mK, showed in a first run a 460 eV FWHM base line and all the features of the $^{241}$Am source used for this experiment (Fig.15).

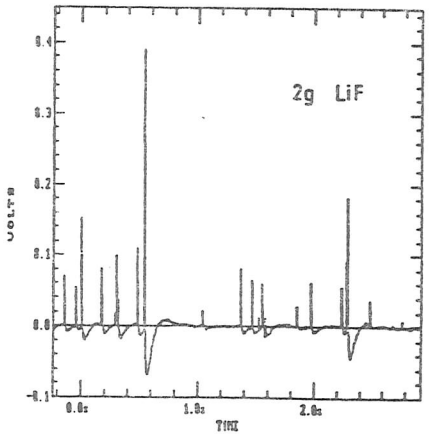


Fig. 16: Pulses from $^{192}$Ir and $^{60}$Co in a 2g LiF bolometer operating at 60mK. The width of the base line was estimated to about 2keV FWHM, after calibration on these sources (IPN, Lyon)

We intend to use it to give definitive results on the hypothesis of cosmions-like particles as has been proposed in our collaboration [9].
A strong argument in favor of bolometer searches for dark matter is the possibility to use different materials, and in particular those which are sensitive to axial coupling ($^{73}$Ge, LiF, NaF,...) [10]. For such a perspective, first results were obtained at IPN (Lyon), using a 2g LiF bolometer, at $T \sim 60$ mK (Fig.16). The internal sources dedicated to nuclear thermometry, $^{60}$Co and $^{192}$Ir, were clearly seen by the crystal, and used for the calibration. A 2 keV FWHM width of the base line is deduced, mainly due to microphonics which should be reduced in a near future.

- - -

Bolometres à Sensen resulty supraconductem :

## Calorimeter with Proximity Effect Thermometer from Probst, Cooper... Seidel 1991

Lower operating temperatures are required for a major improvement of detector performance. The critical temperature of a superconducting film can be reduced via the proximity effect by overlaying it with a film of normal conducting material, such as gold. When both films are pure, or more precisely when the electron mean free path in both materials is larger than the

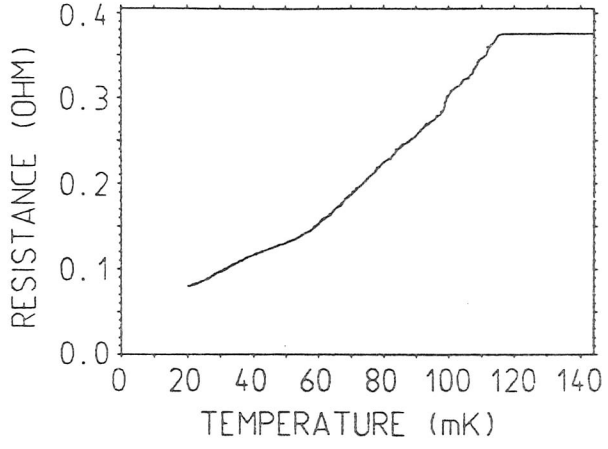


Figure 4: *Temperature dependence of the resistance of the gold-iridium proximity thermometer measured with $I_{ext}$=4 $\mu$A.*

film thickness, the transition temperature depends only on the ratio of film thicknesses for a given pair of materials.

We report here on results obtained with our first calorimeter using an iridium-gold thermometer deposited on a 19 g silicon crystal. The thermometer consists of a 2 mm × 1.0 mm iridium film of 40 nm thickness covered with a larger 2 mm × 1.5 mm gold film of the same thickness and two 800 nm thick gold contact pads. Its transition curve, shown in Fig. 4, is very wide. It starts at about 115 mK and extends below 20 mK. We have already made one proximity structure of the same type on a glass substrate which had a much narrower ($\approx$ 10 mK) transition. A reproducible fabrication of proximity thermometers with narrow transition curves requires more work.

A $^{57}$Co source, emitting 136.5 keV (11%) and 122 keV (89%) photons, was placed outside the dewar to irradiate the detector. A single 122 keV pulse recorded at 25 mK with a read-out current of $I_{ext}$=100 $\mu$A is shown in Fig. 5. The pulse can be well fitted with an exponential rise time of 110 $\mu$s and two exponential decay times of 1.3 ms and about 30 ms. The amplitude of the slow component is very small and contributes less than 2% to the pulse height. The rise time of the pulse is not limited by the electronics.

The contact area between thermometer and absorber consists of a 2 mm$^2$ iridium-silicon interface and a 1 mm$^2$ gold-silicon interface. For the gold-silicon and the iridium-silicon interface we calculate a Kapitza thermal con-

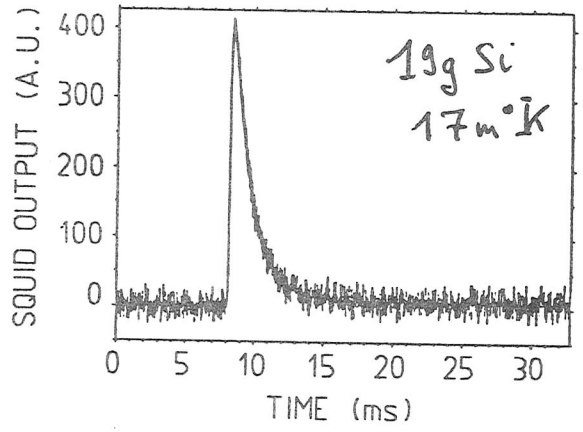


Figure 5: *Single 122 keV pulse recorded with a bandwidth from dc to 50 kHz.*

ductance per unit area of $g_{Ir-Si}$=0.38 $(T/1\mathrm{K})^3$ kW K$^{-1}$ m$^{-2}$ and $g_{Au-Si}$=1.38 $(T/1\mathrm{K})^3$ kW K$^{-1}$ m$^{-2}$, respectively. This gives a thermal coupling between thermometer and absorber of $G_K \approx 33$ nW / K at 25 mK. Using this $G_K$, the thermal conductance of the gold bonding wires of $G_{Au}$ =75 nW / K and a Debye model heat capacity of the silicon-crystal of $C_{Si}$=75 pJ / K we calculate a thermal relaxation time of $\tau = C_{Si}/G_K + C_{Si}/G_{Au} = 3.2$ ms. The rough agreement between $\tau$ and the fast decay time of the pulse (1.3 ms) suggests at first glance that the fast component is a thermal signal. But the amplitude, as discussed in the next paragraph, does not behave as expected for a thermal signal.

One nice feature of the broad transition curve is that it allows us to study the detector response in a wide temperature range. In fig. 6 the temperature rise $\Delta T$ deduced from the full pulse height of 122 keV signals is plotted as a function of the sample holder temperature. The line in fig. 6 represents the temperature rise expected from the heat capacity of the silicon absorber ($\Theta_D$=645 K) and the 122 keV photon energy. The heat capacity of the thermometer is negligible at all temperatures. Signals are larger than expected for a thermal signal at 60 mK and 50 mK and smaller at 25 mK and 17 mK.

Pulses at all operating temperatures were recorded with a read-out current of $I_{ext}$=100 $\mu$A. At the 17 mK operating point about one third of $I_{ext}$ passes through the thermometer dissipating a power of P=110 pW. The influence

of the read-out current heating of the crystal on the photon-induced signal height was tested experimentally by repeating the measurement at the 17 mK operating temperature with a reduced read-out current of $I_{ext}$=30 $\mu$A. The value of $\Delta T$ calculated from the pulse height of this measurement is also plotted in fig. 6. It practically coincides with $\Delta T$ from the experiment at the same sample holder temperature but with eleven times the dissipated power. A heating of the crystal above the sample holder temperature thus can not explain the discrepancy at low temperatures between the data and the temperature rise expected from the heat capacity.

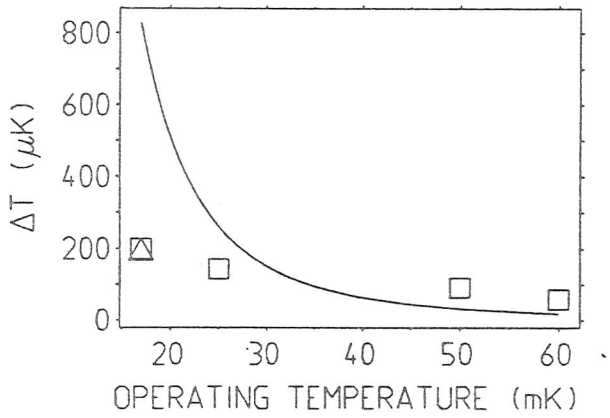


Figure 6: *Full pulse height of 122 keV signals, interpreted as a temperature rise $\Delta T$, plotted as a function of the operating (sample holder) temperature. Squares correspond to a read-out current of $I_{ext}$=100 $\mu$A, the triangle corresponds to $I_{ext}$=30 $\mu$A. The line represents the temperature rise expected from 122 keV $\gamma$ energy and the heat capacity of the 19 g silicon absorber calculated using $\Theta_D$=645 K*

Fig. 7 shows a pulse height spectrum, recorded at an operating temperature of 25 mK with a read-out current of $I_{ext}$=100 $\mu$A. Both the 122 keV and the 136.5 keV $\gamma$ peaks of the $^{57}$Co source can be seen with the expected ratio of counts of about 10:1. Their relative positions agree with the ratio of the $\gamma$ energies and a linear detector response. The fit of a Gaussian curve to the 122 keV peak yields an energy resolution of $\Delta$E=2.3 keV (FWHM).

The spectrum shown in fig. 8 has been recorded with an external $^{241}$Am



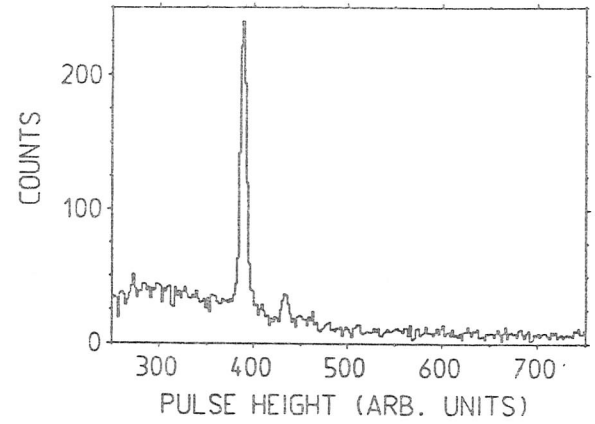


Figure 7: *Pulse height spectrum taken at 25 mK using a $^{57}$Co source, which emits $\gamma$ rays of 136.5 keV (11%) and 122 kev (89%) energy . The source was placed outside the dewar. The width of the 122 keV peak corresponds to an energy resolution of $\Delta E$=2.3 keV (FWHM).*

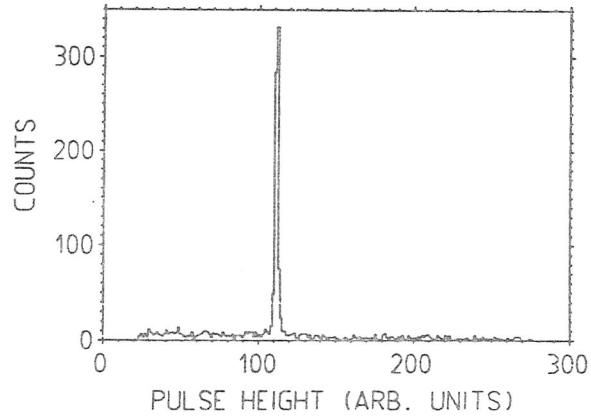


Figure 8: *Pulse height spectrum taken at 17 mK using an $^{241}$Am 60 keV gama source. The width of the 60 keV peak corresponds to an energy resolution of $\Delta E$=1.2 keV (FWHM).*

60 keV $\gamma$-source at a lower operating temperature of 17 mK and an optimized read out current of $I_{ext}$=110$\mu$A. A Gaussian curve fitted to the peak yields an energy resolution of $\Delta$E=1.2 keV (FWHM).

A more narrow transition should considerably improve detector performance. We believe this can be achieved with better deposition and structuring techniques. Another possibility is to use tungsten, which has a bulk transition temperature of 15 mK. We plan to pursue both possibilities in parallel.

## References


[1] W. Seidel, G. Forster, W. Christen, F. von Feilitzsch, H. Göbel, F. Pröbst and R. L. Mößbauer, Phys. Lett. B 236 (1990) 483.

[2] S. Tamura, Phys. Rev. B 1985 2574, and Phys. Rev. B 30 (1984) 849

[3] Th. Peterreins, J. Jochum, F. Pröbst, F. von Feilitzsch, H. Kraus, an R. L. Mössbauer J. Appl. Phys. 69 (1991) 1791

# Resultats de Fiorini et al à Milan

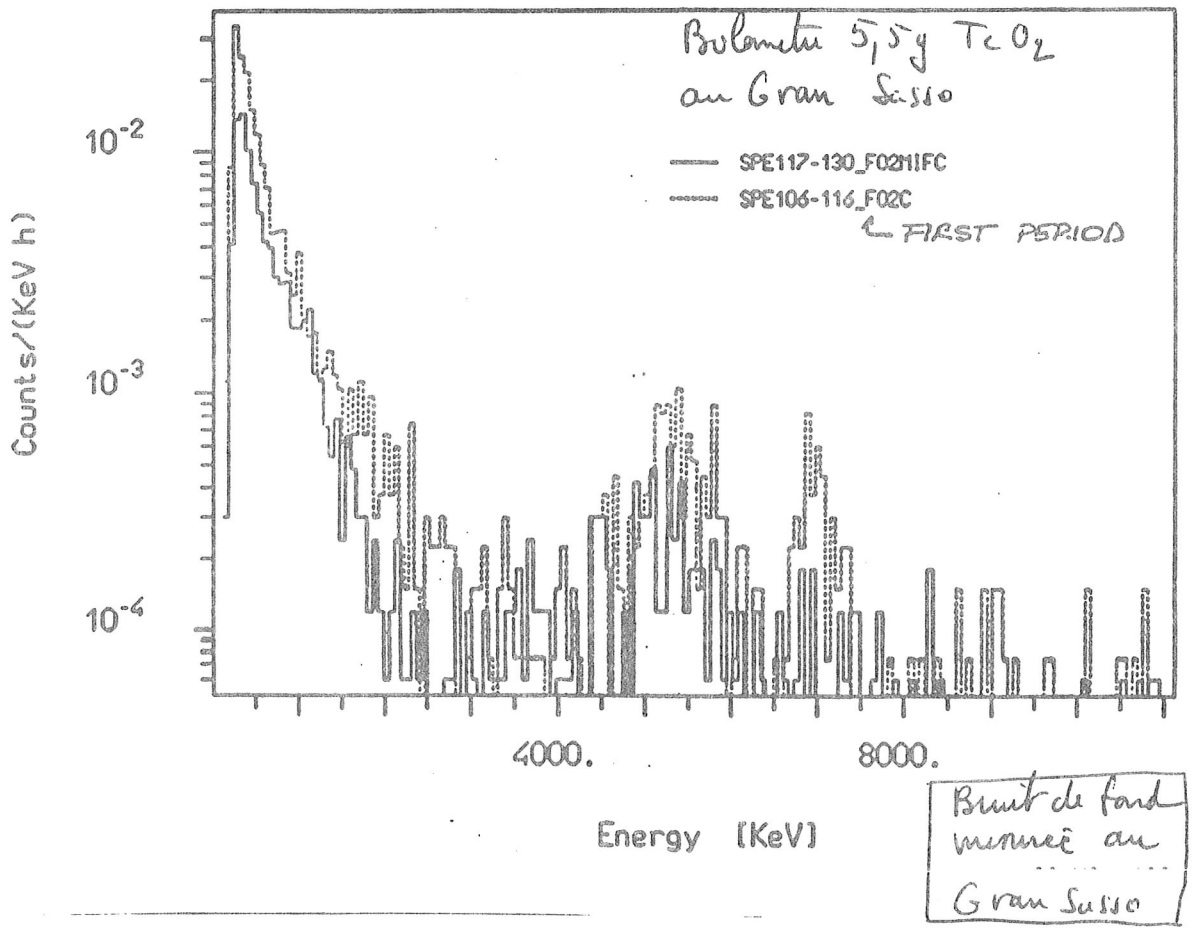


Bruit de fond mesuré au Gran Sasso

## • NTD Ge RADIOACTIVE PROPERTIES

- PRESENCE OF RELATIVELY LONG LIVED $\gamma$ & $\beta$ EMITTERS PRODUCED BY (FAST) n REACTIONS ON Ge ISOTOPES AND IMPURITIES
- NON NEGLIGIBLE CONTRIBUTIONS EVEN FEW YEARS AFTER IRRADIATION ESPECIALLY AT LOW ENERGIES (DARK MATTER)
- $E_0$ ($^{68}$Ga) = 1.9 MeV ⇝ $\beta\beta_{2\nu}$

⇝ SIGNAL DISCRIMINATION ?

← etude des impuretés radioactives dans les NTD Ge

## • $\beta\beta$ DECAY OF Tellurium

- GOOD RESULTS ALREADY ACHIEVED WITH A 5.5 g $TeO_2$ BOLOMETER

$B_{\beta\beta} = 8 \cdot 10^{-5}$ c/keV/h.

$$S = \ln 2 \frac{N_{Te^{130}} \cdot \varepsilon \cdot T}{\sqrt{B_{\beta\beta} \cdot FWHM \cdot T}} = 3 \cdot 10^{20} \text{ y} \quad (T = 1\text{y})$$

$t_{1/2}$ (PRELIMINAR) $> 3 \cdot 10^{19}$ yrs

← premier résultat sur $\beta\beta$ decay de Te avec un bolometre

- **FUTURE** 1. $TeC_2$ ARRAY (500 g)
2. $CaF_2$ : $\alpha$-$\beta$ DISCRIMINATION PROGRAM

Exp 342 nov 1991 LSM
24g $Al_2O_3$ vu 10h30
(dérives post-pulses soustraites)
imax > 5000

Filtre 1.342
[filtre 15kg - 35kg appliqué

Vmax - Vmin
Calib. d'après 122 keV

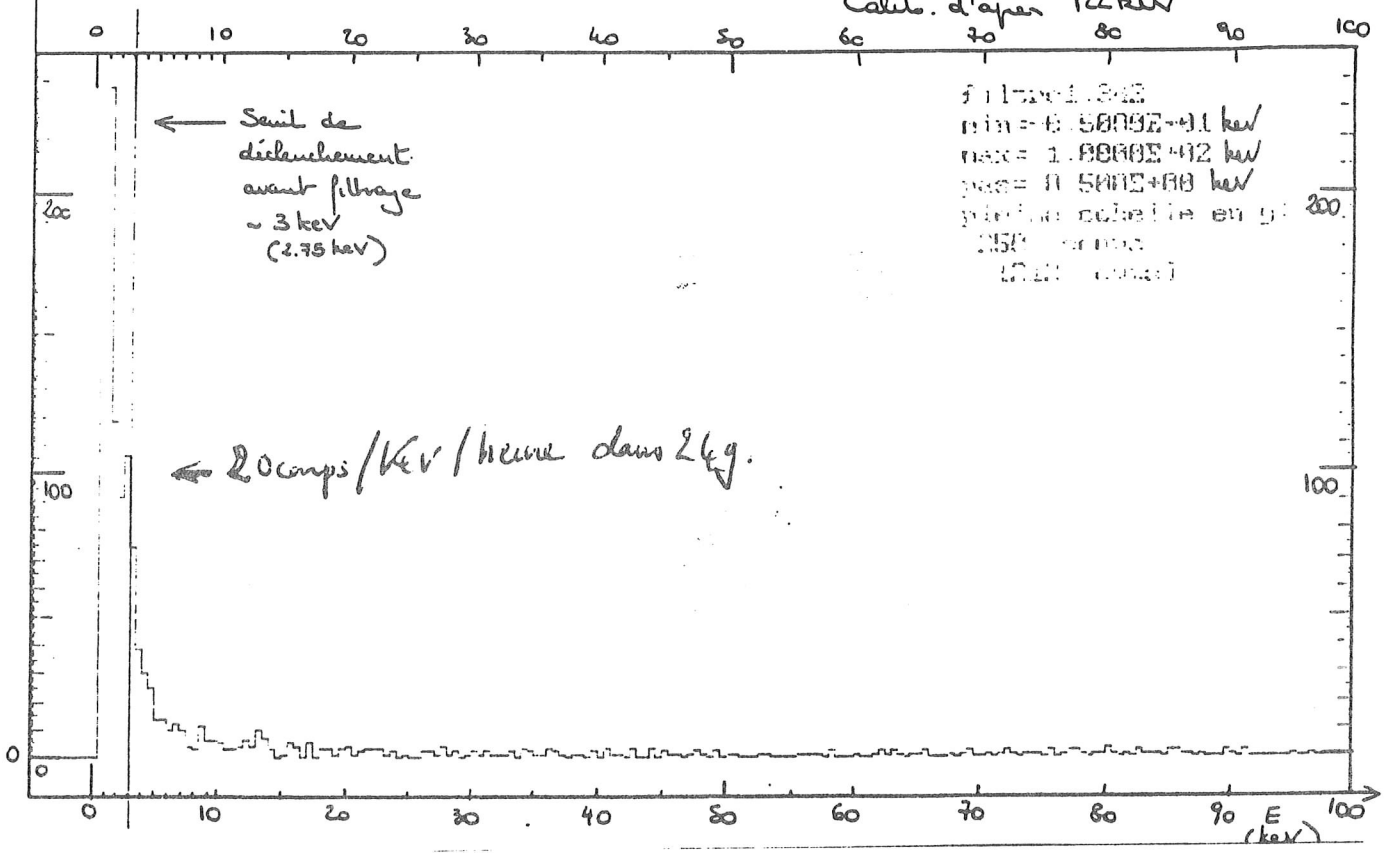


EXP 342 (suite)
(00)
{ Calibration d'après 122 keV
hypothèse : linéarité

durée ~ 10h
[596 mn]

Exp 346
do
$Al_2O_3$ uniquement
(sélection sur trive)

Vmax

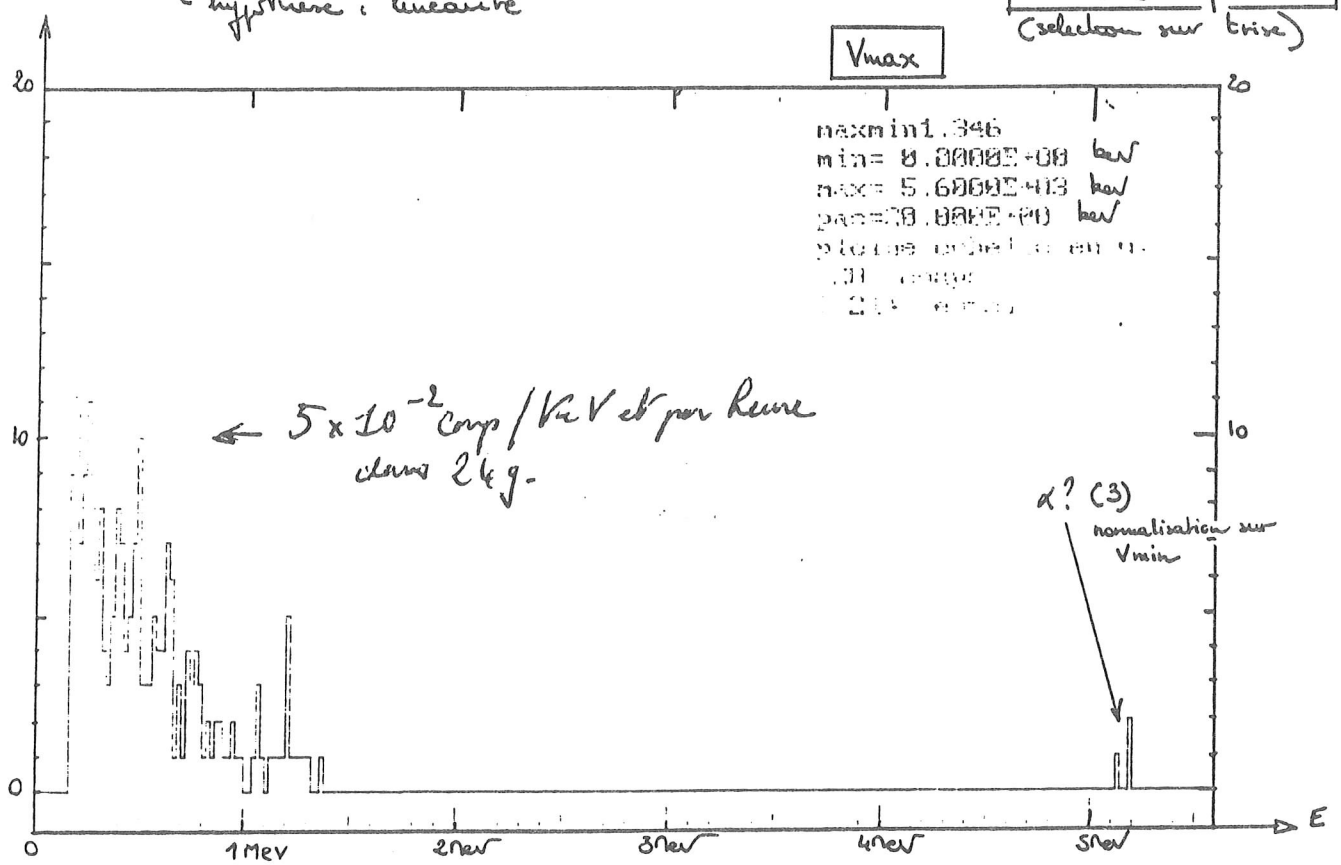


- Résultats obtenus à Modane avec 24g. $Al_2O_3$ — (Pole Marcillac et al.)